ADDIS ABABA UNIVERSITY

SCHOOL OF GRADUATE STUDIES

SCHOOL OF EARTH SCIENCE

METAMORPHISM, DEFORMATION HISTORY AND GEOCHEMISTRY OF NEOPROTEROZOIC ROCKS OF WORKAMBA AREA, TIGRAY NORTHEREN ETHIOIPIA

BY

WULETAW MULUALEM

A thesis submitted to School of Graduate Studies of Addis Ababa University, in partial fulfillment of the requirements for the degree of Master of Earth Science (Petrology)

May 2017

ADDIS ABABA UNIVERSITY
SCHOOL OF GRADUATE STUDIES
SCHOOL OF EARTH SCIENCE

METAMORPHISM, DEFORMATION HISTORY AND GEOCHEMISTRY OF NEOPROTEROZOIC ROCKS OF WORKAMBA AREA, TIGRAY NORTHEREN ETHIOIPIA

BY

WULETAW MULUALEM

ADVISOR: MULUGETA ALENE (PhD)

A thesis submitted to School of Graduate Studies of Addis Ababa University, in partial fulfillment of the requirements for the degree of Master of Earth Science (Petrology)

May 2017

ADDIS ABABA UNIVERSITY

SCHOOL OF GRADUATE STUDIES

SCHOOL OF EARTH SCIENCE

METAMORPHISM, DEFORMATION HISTORY AND GEOCHEMISTRY OF NEOPROTEROZOIC ROCKS OF WORKAMBA AREA, TIGRAY NORTHEREN ETHIOIPIA

BY

WULETAW MULUALEM

Approved by the Examining Committee	**Signature**	Date
Dr. Balemwal Atnafu	……	……...
Head, School of Earth Sciences		
Dr. Mulugeta Alene	……	.……
Advisor		
Prof. Dereje Ayalew	……	……..
Examiner		
Prof. Gezahegn Yirgu	…….	……
Examiner		

ACKNOWLEDGMENT

I am deeply grateful to Dr. Mulugeta Alene my advisor who gave me continuous guidance, constructive comment and suggestion and also for his interest to technical discussion and encouragement to me from the beginning to the end of my study.

I would like to thank very much Addis Ababa University, School of Earth Sciences for funding this project.

I run out of words to express my deepest thank to ato Wondowessen who helped me in works gleefully during geochemical samples cutting processes.

My special thanks also go to my dear parents, colleagues and friends for their great support and for their helpful suggestions.

Last but not least, thanks are also extended to the community of Workamba town for their impressive support, especially ato Kasay G/Selassie who helped me during field work to carry out the field mapping go smoothly.

DECLARATION OF ORIGINALITY

This is my original work and has not been presented for a degree in any other University, and that of all sources of material used for the thesis have been dully acknowledged.

Wuletaw Mulualem

TABLE OF CONTENTS

Contents

LIST OF FIGURES

LIST OF TABLES

ABSTRACT

The Workamba area is situated within Northern Ethiopia and covered by widely distributed metavolcano-sedimentary Neoproterozoic basement rocks which belong to the Tsaliet and Tambien Groups in the southern part of Arabian Nubian Shield (ANS). In this study the integrated petrographic, structural kinematics and geochemical analysis has been carried out to understand the metamorphism, deformation history and geochemistry of the area.

The foliated and nonfoliated metabasics, metabasaltic-andesite with intercalation of tuffaceous layer, metavolcanoclastic and metabreccia rock units are characterize the Tsaliet Group whreas, metasedimentary rock units include; metalimestone, graphitic slate, phyllite and micaceous slate are represent the Tembain group. The index mineral assemblages such as chlorite, actinolite, epidote, muscovite and serisite which established from petrographic analysis indicate that the study area has been experienced low grade metamorphism (green schist facies metamorphism). Petrographic, macro and micro scale geologic structure studies show that the study area has experienced two phases of ductile deformation (D1 and D2) and later affected by third phase brittle deformation. Metamorphism-deformation relationships are recognized from mineral assemblages and micro-structural features. D1 is established by NE striking S1foliation and regional M1 metamorphic event synchronous with D1 is responsible for development of mineral assemblages such as chlorite, epidote, actinolite, muscovite/sericite, calcite, graphite and recrystallized quartz. The second phase deformation (D2) is characterized by the local development of low plunging folds, S2 cleavage and kink fold. During D2 deformation S1foliation is folded to S2 crenulation cleavage by slightly rotation and recrystallization of platy minerals i.e., micas therefore S2 cleavage can be accommodate by M2 metamorphic event synchronous with D2 deformation. The third phase deformation (D3) is related to different set of joints that cross cut the regional foliation throughout each rock units. The geochemical data plotted on different tectonic discrimination diagrams clearly reveals that metavolcanic rocks of Workamba area are characterized by typical calc-alkaline suites. The general petrological and geochemical characteristics of the Workamba metavolcanic rocks provides an important evidence to consider the area as part of the arc volcanics sequence or subduction-related arc accretion of the ANS.

CHAPTER ONE

1. INTRODUCTION

1.1 BAGROUND INFORMATION

Within the Pan-African domains, Orogenic belts of the Arabian Nubian Shield (ANS) and the Mozambique Belt (MB) are believed to be more prominent in outcrop in Ethiopia than in any other country of the Horn of Africa (Kazmin, 1972; Berhe, 1990). However, the rocks belonging to these orogenic belts are only exposed in a few areas, which have not been affected by Cenozoic volcanism and rifting, and where the Phanerozoic cover rocks have been eroded away (Tefera et al., 1996).

The Northern metamorphic terrain of Ethiopia consists of a series of thick, inhomogeneous volcano-sedimentary assemblages that belong to the ANS of the Pan-African orogen (900---500 Ma), (Asrat et al., 2004).

The Arabian-Nubian Shield (ANS) in NE Africa and W. Arabia is the largest tract of juvenile continental crust of Neoproterozoic age on Earth (Patchett and Chase, 2002, cited in Stern et al.,2004).

The ANS (Fig.1.1) makes up the northern half of the East African orogeny (EAO) and extends from southern Israel and Jordan south as far as Ethiopia and Yemen, where the ANS transitions into the Mozambique Belt (Berhe, 1990; Kroner et al., 1991; Stern, 1994; Teklay et al., 1998, 2001 and Stern, R.J., Kroner, A., 2005).

Beyth (1972) broadly subdivided the low-grade basement rocks in Tigrai region into two the Tsaliet and Tembien Groups based on stratigraphical relationships. The Tsaliet Group is older among the two and covers most area of the region occupied by basement rocks. The Tsaliet metavolcanics are formed mainly of intermediate to acidic tuff, lapilli tuff, agglomerate which are very well bedded and with limestone at their upper part.

Tambien Group on the other hand is mainly exposed in a series of synclinal inliers overlying the Tsaliet Group with gradational contact from west to east Maikenetal, Tsedia, Chehmit, and Negash (Alene et al., 2006; Garland, 1980). It consists of metasedimentary rocks of argillite and carbonate composition but predominantly argillaceous. The rock types present are slate, phyllite, graphitic schist greywacke, metalimestone and quarzo dolomite.

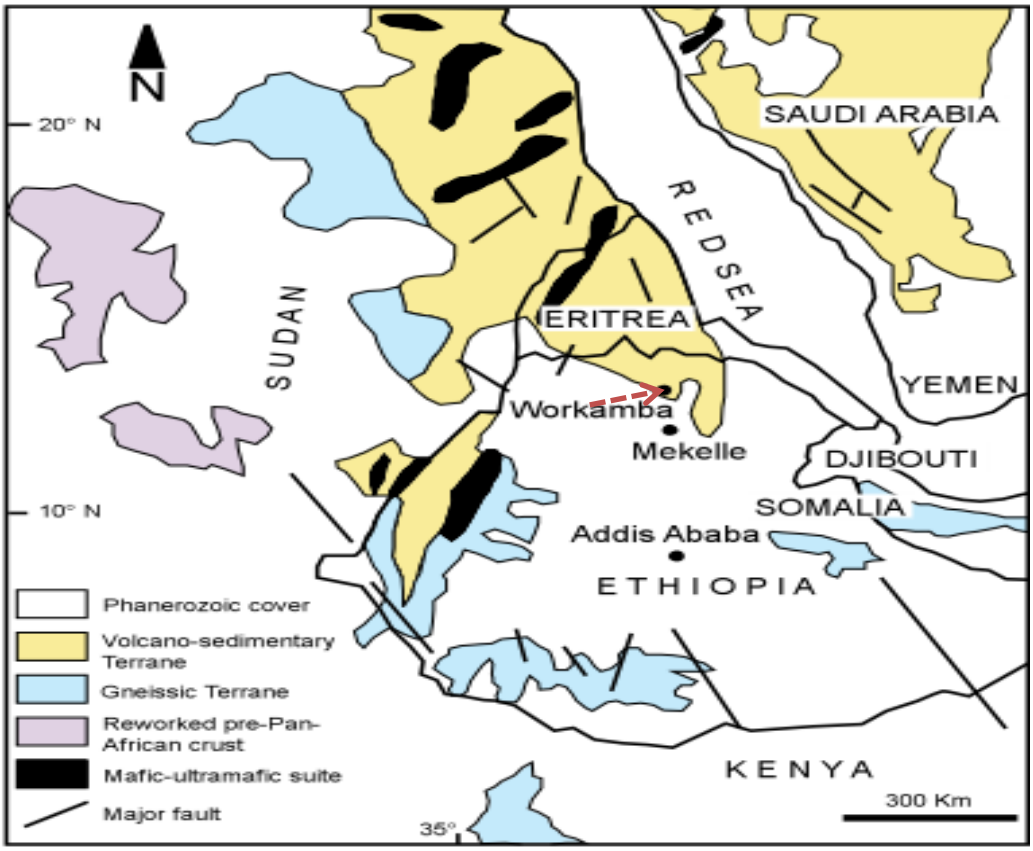

Figure1.1 Distribution of rocks of the Arabian-Nubian Shield, which form the basement rocks Arabian Peninsula, Northeast Africa (Egypt and Sudan), and Ethiopia, showing general geology and distribution of volcano-sedimentary exposures and the study area localities within ANS (After Ayalew et al., 1990; Berhe,1990; Asrat et al., 2001; Solomon ,2009).

The tectonic structures recorded by the Tsaliet and Tambien group rocks are related to the ANS that developed during the Neoproterozoic by rifting, arc accretion and terrain amalgamation processes in the East African Orogen (Stern, 1994; Meert,2003; Johnson and Woldehaimanot, 2003). Two phases of deformation (D1 and D2) are recognized in parts of the Tsaliet and Tambien Group rock units (e.g. Alene, 1998). Deformation D1 is caused by N-S compression and resulted in tight minor folds with a wavelength of several mm to dm, elongation lineation and pervasive regional foliation. D2 deformation resulted from E-W directed compression at the waning stage of the collision between East and West Gondwana and yielded long wave length (about 8 km), upright, open parallel folds without a significant cleavage, thrust, and strike slip faulting, (Alene, 1998; Alene et al., 2006).

ANS in Ethiopia which is dominantly exposed in northern part of the country (Kazmin, 1973; Asrat et al, 2001) (see also Fig.1.1), is mantle-derived juvenile continental crust formed by subduction-related arc accretion (e.g. Tadesse et al., 1999; Avigad et al., 2007).

The Petrological, structural and geochemical, study of both Tsaliet and Tembien groups in northern Ethiopia appears to be the best ways to understand the geodynamic evolution of those volcano-sedimentary rocks and to characterize grade of metamorphism.

1.2 Problem Statement

In Northern Ethiopia the previous researchers have identified and mapped extensive low grade Neoproterozoic basement rocks comprising metavolcanic, metasediments and intrusive of various composition. The metamorphic rocks were given formal stratigraphic names and were correlated with the low grade of western and southern Ethiopia (Beyth, 1972; Kazmin, 1972).

According to the previous workers (Beyth, 1972; Kazmin, 1972; Mengesha, et al., 1996) most part of the Precambrian rocks of northern Ethiopia belongs to two major stratigraphic groups (the Tsaliet and Tembien groups) with minor but locally important younger stratigraphic formation namely Didikama formation, the Shiraro formation and Matheows formation in younging stratigraphic sequences.

The two major sequences, the Tsaliet and Tambien Groups have received good deal of scientific attention by many researchers. More recently, several regional scale geological studies or studies on specific aspects were conducted (e.g. Alene 1998; Alene et al., 2000, 2006; Asrat 2002; Swanson-Hysell et al., 2015; Tadesse 1996; Tadesse et al., 1999, 2000; Miller et al., 2003; Stern et al., 2005).

Further works has not been done on Workamba area. Therefore to have better understanding of this area in metamorphism and deformation history; detail mapping of lithology, petrographic and geochemical studies of rocks with field observations are important.

1.3 Significance of the Study

As mentioned earlier previous the researchers have identified and mapped extensively low grade Neoproterozoic basement rocks comprising metavolcanic, metasediments and intrusive of various composition. But detailed work at a scale of 1:25,000 has not been done in the Workamba area.

This work consists of a detailed mapping at a scale of 1:25,000, and includes deeper understanding of the petrography, deformation phases and geochemistry of the area. This in turn

is believed to contribute in the interpretation and elucidation of regional geology and Neoproterozoic tectonics. The new data could also serve as a basis for further geological studies and resource exploration in the area.

1.4 Location and Accessibility of Study Area

The study area is located100 km northwest of Mekelle around werkamba, central Tigrai northern Ethiopia which is about 900km north of Addis Ababa and it covers ~88km^2. Geographically it bounded between 0494000-050500E and 1520000-1528000N UTM coordinates (Fig.1.2B). It is accessed through the main asphalt road from Mekelle through Hawzen and toWerkamba.

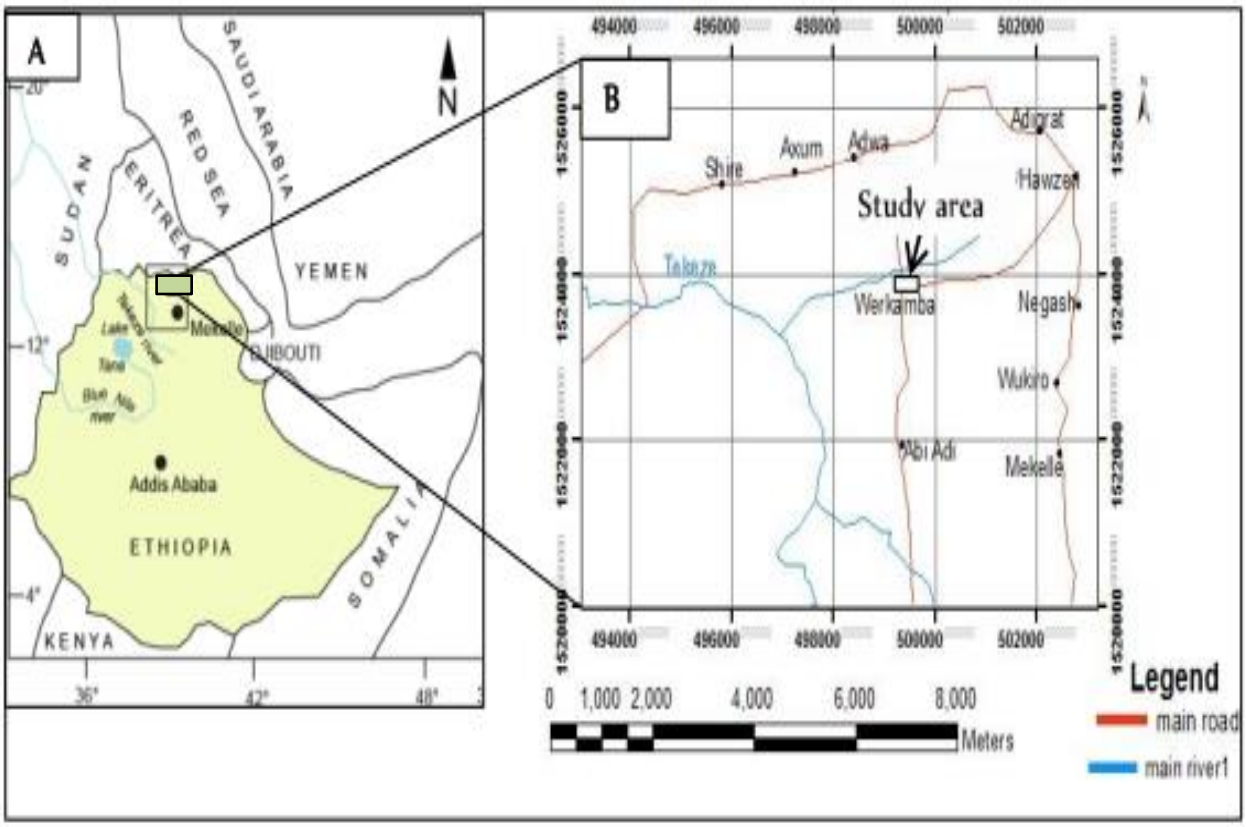

Figure1. 2 Location and accessibility map of the study area (Inset rectangle) in the left side figure 1.2 A and in the right figure 1.2B in northern Ethiopia.

1.5 Physiography and climate of the Study Area

The study area is characterized by rugged topography and slightly flat topographic feature in south east and the Eastern parts. The drainage pattern of the study area is mainly accomplished

by the perennial Tsaliet River and its tributaries. The study area is categorized under arid to semi-arid receiving an annual rainfall of 678-1286 mm and the main rainy season is from June to August and the temperature ranges from 11^{o}C in a cold season to 33°C in a hot season (Tigray Meteorological Agency, 2010).The population of the area is sparsely settled and their main source of income is agriculture.

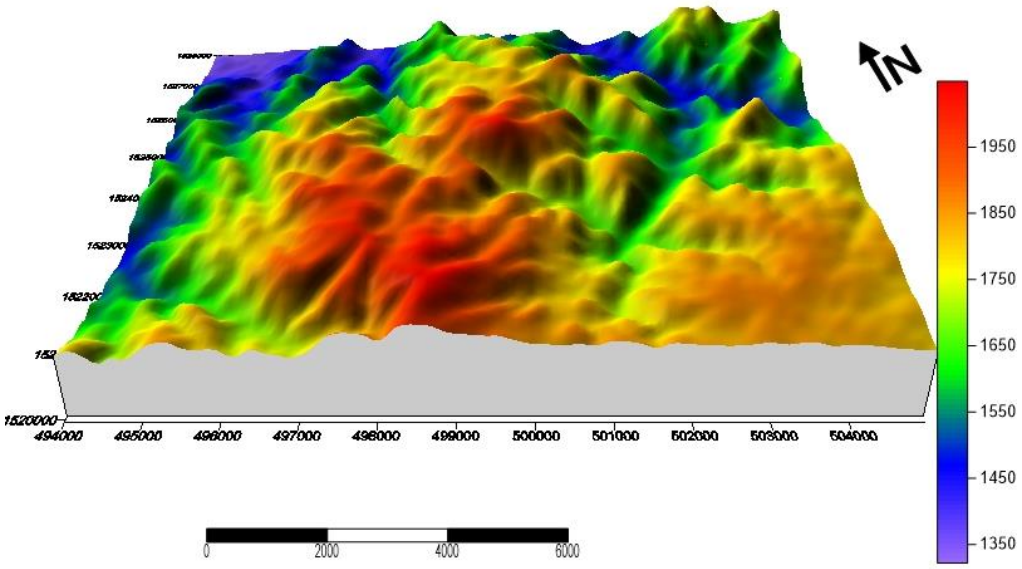

Figure 1.3 Physiography map of the study area. The area is characterized by rugged topography and slightly flat feature in south east and the Eastern parts.

1.6 Objectives

1.6.1 General Objective

The main objective of the study is to describe and understand the metamorphism, deformation history, the nature of mineral transformation under the effect of dynamic deformation and geochemistry of Workamba area, central Tigray, northern Ethiopia.

1.6.2 Specific Objectives

- To examine the rock fabric and determine the metamorphic facies,
- Description and analysis of macro and micro scale geologic structures of the area,
- To recognize and differentiate phases of deformation and metamorphism,
- To evaluate and understand the geochemistry of the study area
- To produce a geologic map of the study area at scale of 1:25,000

1.7 Methodology

1.7.1 Field work and Geological mapping

Methodologies which were employed to accomplish the above objectives have been divided in to three stages; pre-field work, field work and post-field work. Collection of secondary data literature review and obtaining of materials and instruments used during field work were made in the pre-field work stage.

During field work collection of fresh samples from each lithological unit for thin section and geochemical analysis, producing geological map at the scale of 1:25,000, description of the rock units and structural measurements were carried out. Post-field work includes analyzing, synthesizing, presenting and interpreting of data.

1.7.2 Petrographic Analysis

Twenty one rock thin section samples are prepared in Geological Survey of Ethiopia and they have been examined, at the School of Earth Sciences, Addis Ababa University for metamorphic mineral assemblage, fabric identification as well as for microstructural and micro-texture analysis.

1.7.3 Structural Data Analysis

Field structural data was compiled using Arc GIS software to produce geologic map at scale of 1:25,000, which shows lithological units and orientations of major geological structures. Stereo graphic projection is also used to analyze structural elements associated with each phase of deformation.

1.7.4 Geochemical analysis

Twelve representative rock samples have been selected from different lithological units for geochemical analysis. The analytical techniques for major, trace and rare earth elements has been carried by inductively coupled plasma mass spectrometry (ICP-MS) and inductively coupled plasma-atomic emission spectroscopy(ICP-AES)technique at Australia laboratory science (**ALS)** Geochemistry.

1.7.5 Review of Previous Work

The first recorded geological work in the northern province of Ethiopia was done by Blanford (1870) as sited by Beyth (1972). After this time different geological mapping were carried out by different researchers.

The basement rocks in northern Ethiopia were grouped under an Upper complex division of the three fold classification of Ethiopian basement rocks, based on metamorphic and structural complexities (Kazmin 1973; Kazmin et al. 1978). These rocks are characterized by the occurrence of low-grade variety of sedimentary, volcanic and intrusive rocks which have been metamorphosed (Beyth, 1972; Kazmin, 1972).

Kazmin et al. (1978) have divided the Precambrian basement of Ethiopia in to Upper, Middle and Lower Complexes based on compositional, deformational and metamorphic grade variations. They also considered as the Upper Complex rocks to be Late Proterozoic in age, Middle and Lower Complexes to be Middle and Early Proterozoic (or Late Archean). But recent studies on the basis of the geochronological and isotopic data (Gerra, 2000, Teklay et al., 1998 and others) have suggested that the Precambrian basement rocks are dominantly Neoproterozoic in age and have experienced different grades of metamorphism. The Precambrian geology of Ethiopia consists of two distinct lithotectonic terranes which show contrasting lithological association, internal structures and grade of metamorphism (Yibas et al., 2000).

The new subdivision of Ethiopian basement rock is composed of two major blocks: (i) a gneissic and migmatic terrain, which essentially consists of the Lower and Middle Complex and correlated with the Mozambique Belt; (ii) a low-grade volcano-sedimentary terrain, which comprises all the rocks of the Upper Complex and is correlated with the ANS. Pre-, syn-, and post-tectonic granitoids intruded the Ethiopian basement rocks (Asrat et al. 2001).

The stratigraphy framework of the Neoproterozoic low-grade basement rocks of northern Ethiopia was described by Beyth (1972). He divided these basement rocks into Tsaliet and Tambien Groups. Tsaliet Group is dominated by metavolcanics and metavolcaniclastics units and the overlying Tambien Group which consists of shallow marine metasedimentary succession of slates, phyllites, greywacke and carbonates (Beyth, 1972; Kazmin, 1973; Tadesse, 1996; Alene, 1998; Beyth et al, 2003; Alene et al., 2006). The Tambien Group in centeral Tigray is exposed in a series of four synclinal inliers, surrounded by the Tsaliet Group rocks and these four synclinoria are from west to east: Mai-Kenetal,Tsedia, Chehmit, and Negash inliers (Beyth 1972; Alene et al. 2006).The metamorphic grade of the Tsaliet metavolcanics and the Tambien Group is low and, except around intrusions, never rises above greens chist facies (Alene, 1998; Alene and Sacchi, 2000; Beyth e al., 2003).

The geochemistry of the volcanic rocks in some northern Ethiopian region is characteristically calcalkaline, and most yield arc-related geochemical signatures. Such calcalkaline volcanic activity, post-orogenic granitoids and deposition of clastic rocks are common in the juvenile crust of the ANS (Sifeta et al., 2005).

The basement rocks of Ethiopia have long been considered to be part of the Arabian–Nubian Shield (Kazmin et al., 1978; Tadesse et al., 1999; Asrat et al., 2001).

The structure of the basement complex is defined by NE-trending folds with NW-dipping bedding and foliation on the plateau, and SE-dipping structure in the Ethiopian escarpment area (Beyth et al., 2003). The tectonic structures recorded by the Tsaliet and Tambien Group rocks are related to the collisional stress that resulted in the amalgamation of the ANS. Generally, two phases of deformation (D1 and D2) are recognized (Alene et al., 2006).

This study aims to contribute detail petrographic, structural and geochemical data about the area to improve existing knowledge and metamorphism, structural and geochemical correlation has been done with regional works.

CHAPTER TWO

2. REGIONAL GEOLOGY

2.1 Regional Geologic setting

2.1.1 Geodynamic evolution of the East African Orogen

Stern (1994) coined the term East African Orogen (EAO) for both the combined upper crustal Arabian-Nubian Shield (ANS) and lower crustal Mozambique Belt (MB). EAO represents a plate tectonic cycle spanning a time-period of 350 Ma, beginning by about 900 Ma with rifting and continental break-up and ending by about 550 Ma subsequent to a continent-to- continent convergence between East and West Gondwana (Vail, 1985; Berhe, 1990; Abdelsalam and Stern, 1996).

The EAO developed due to the collision of East and West Gondwana (Fig. 2.1) during the late Proterozoic, which finally formed the Gondwana Supercontinent (de Wit and Chewaka 1981; Stern 1994; Stern 2002; Stern et al. 2005). The EAO also represents one of Earth's greatest collision zones, which is about 6000km long. The tectonic evolution of the East African Orogen are: (i) Rodinia rifting and break-up at~900-850 Ma; (ii) seafloor spreading, arc and back-arc basin formation, and terrane accretion from 870 to 690 Ma; (iii) continent-continent collision from 630 to 600 Ma, and(iv) further crustal shortening, orogenic collapse and extension leading to the break-up of Gondwana during 600 to 540 Ma (de Wit and Chewaka 1981; Stern 1994; Stern et al., 2006).

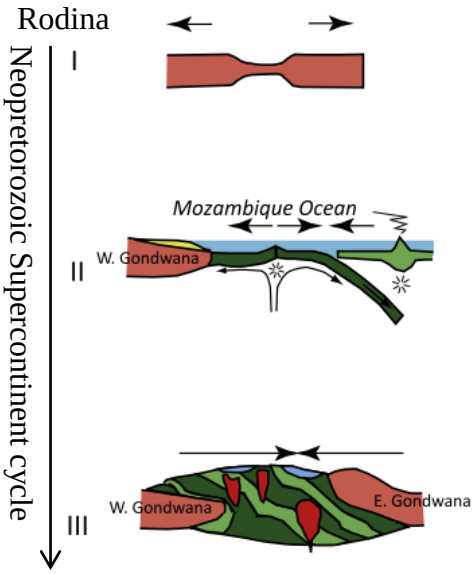

Rifting and break-up of Rodina:
Initiation of Mozambique ocean
870-800Ma.

Juvenile crust production:
Sea-floor spreading and arc and back arc formation, followed by terrain accretion
800-670 Ma.

Crustal and lithospheric reworking:
Continental collision forming the East Africa Orogen; granitic Magmatism, and post-amalgmation volcanic-sedimentary deposition
650-600 Ma.

Crustal and lithospheric reworking:
continued shortening, deposition and magmatism escape tectonics and orogenic collapse
600-650 Ma.

Figure 2.1Tectonic evolution of the East African Orogen that resulted in the greater Gondwana Super continent (after Johnson et al., 2011). W.G=West Gondwana and E.G=East Gondwana.

2.1.2 Mozambique belt

Mozambique Belt (MB) is the southern part of the East African Orogeny and essentially consists of medium to high-grade gneisses and voluminous granitoids and it extends south from the Arabian-Nubian Shield into southern Ethiopia, Kenya and Somalia via Tanzania to Malawi and Mozambique and also includes Madagascar (Kroner and Stern, 2005).There is no overall model for the evolution of the MB although most workers agree that it resulted from collision between East and West Gondwana. Compared to the strong deformation and metamorphism experienced during collision in the Mozambique belt, the ANS was considerably less affected by the collision. The Mozambique Belt exposes higher temperature and pressure suites with abundant amphibolite and granulite-facies metamorphic rocks and gneiss terranes (Avigad et al. 2007).

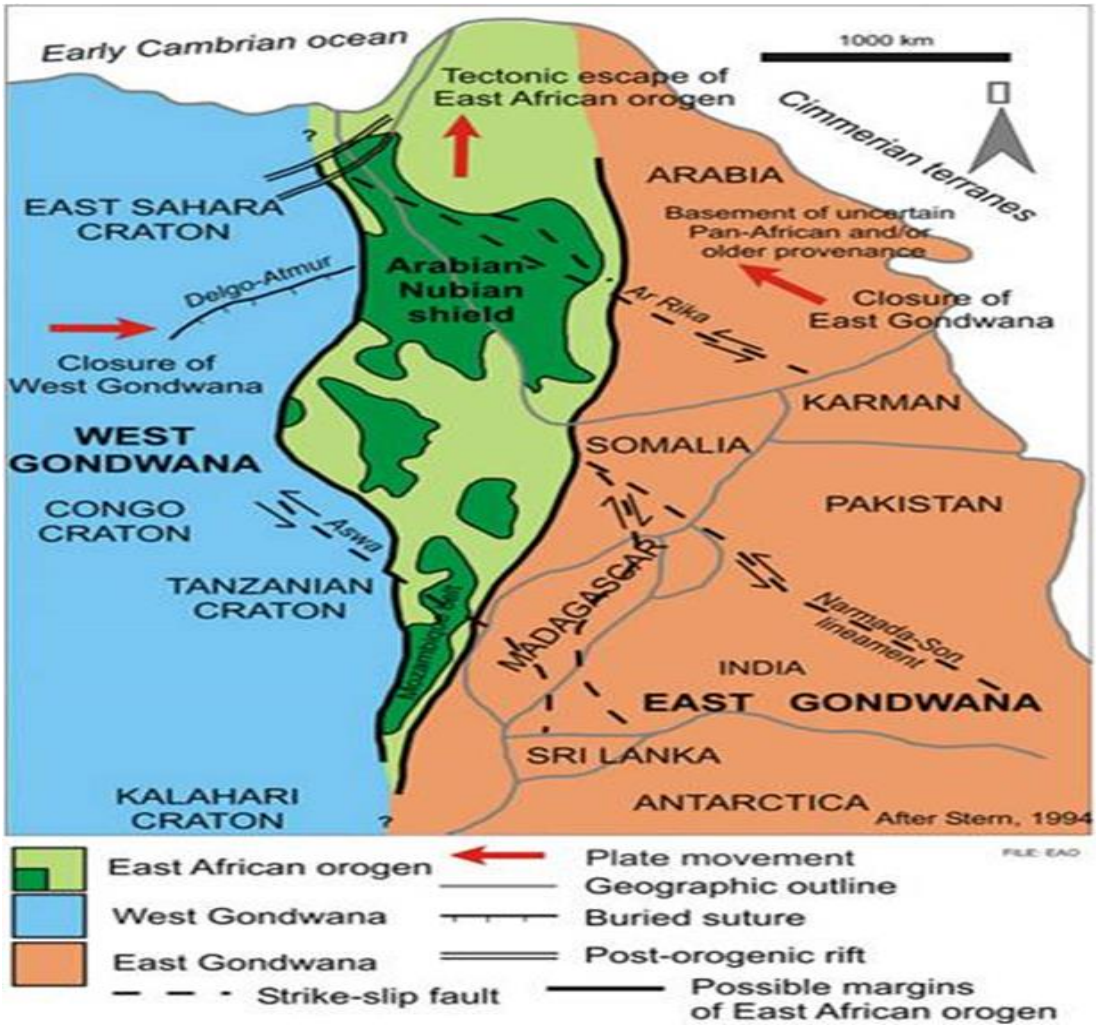

Figure 2.2 Map of the East African Orogen showing the location of the Arabian-Nubian Shield relative to the Mozambique Belt and adjacent cratonic margins (after Stern 1994).

2.1.3 The Arabian Nubian Shield

The Arabian-Nubian Shield (ANS) was formed at the end of Neoproterozoic time when east and west Gondwana collided to form the supercontinent Gondwana (Vail, 1985; Stoeser and Camp, 1985 Johnson, 2011 and 2014) and consists of Precambrian rocks exposed on either side of the Red Sea in westem Arabia and northeastern Africa (Fig.2.3). It mainly consists of sutured low grade assemblages of Neoproterozoic volcanic, volcano sedimentary and sedimentary units, intrusive and contains many remnants of oceanic crust in the form of ophiolites (Abdesalam and Stern, 1996; Tadesse, 1996; Alemu, 1998).

The EAO (Stern, 1994; Kusky et al., 2003) consists of deformed and metamorphosed low grade rocks of the ANS in the north and higher grade and more strongly deformed rocks of East Africa and Madagascar in the south. These high grade rocks were derived from continental crust recycled during the East African Orogen, greenschist to lower amphibolite metamorphosed volcano-sedimentary terranes including calc-alkaline basaltic and andestic lavas, tuffs, pyroclastics, and rhyolites, which are intruded by various pre-, syn-, and post-tectonic granitoids and occurring between the western and eastern gneissic terrain (Vail 1985).

Abdelsalam and Stern (1996) recognized two deformation belts in the ANS: (1) Related to arc-arc and arc-continent collision, which are both associated with sutures. The arc-arc deformation belts are manifested by the occurrence of E-W and N-S verging ophiolities in the northern and southern parts of the ANS respectively. The E-W verging ophiolities are steepened by upright folds, whereas those of N-S vergence are deformed by up-right folds and strike slip faults related to oblique collision of the terranes at about 800-700 Ma. The arc-continent deformation belts are related to the collision of East and West Gondwana. (2) Post-accretionary structures (~650-550 Ma) resulted from continuous shortening of the ANS and developed NW trending strike slip faults and shear zones during the waning stages of ANS formation. According to Avigad et al.,(2007), Northern Ethiopia (Tigray) and much of Eritrea and Ethiopia plateaus expose ANS-type green-schist facies volcano-sedimentary sequences.

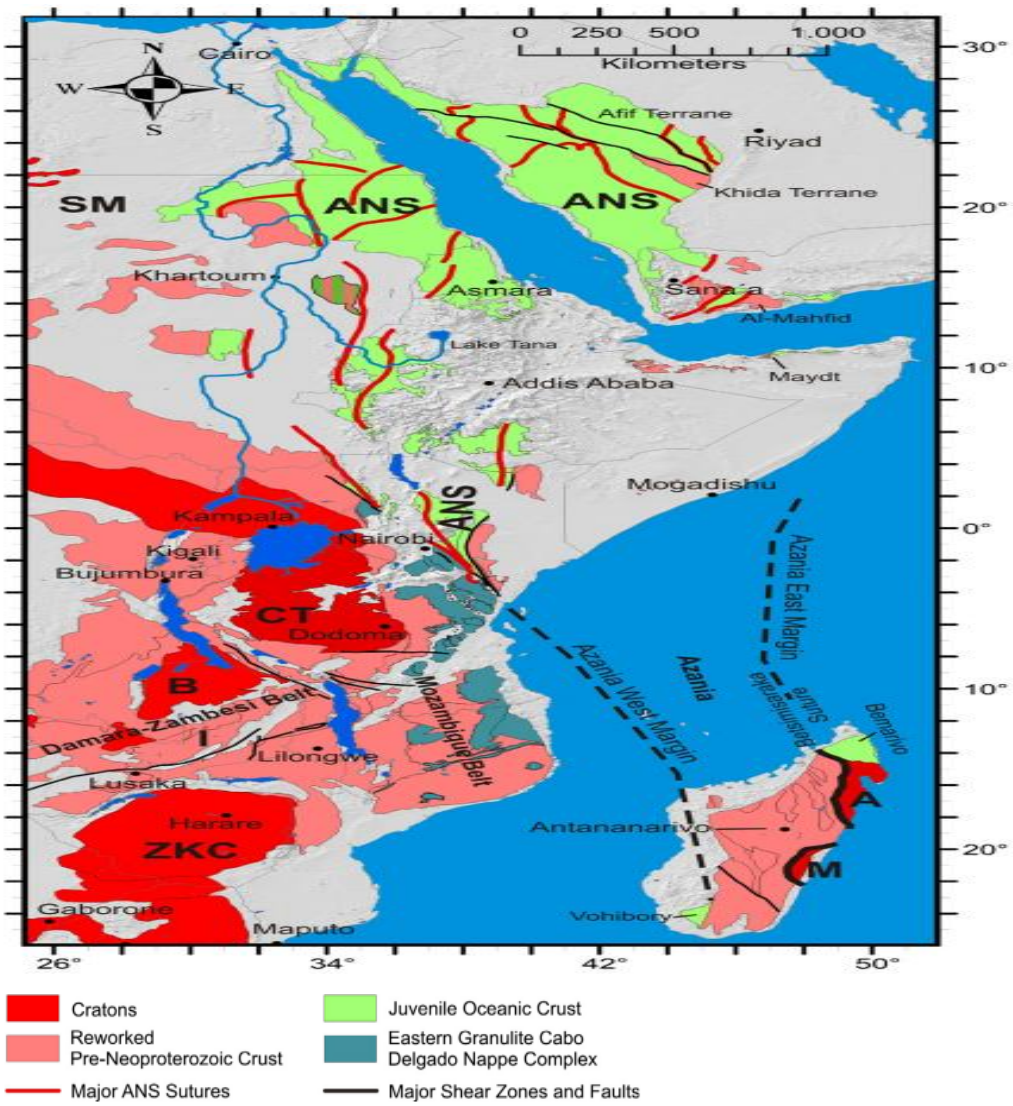

Figure 2.3 The Arabian–Nubian Shield in relation to East Africa as component parts of the East African Orogenthat extends as far south as southern Kenya and northern Ethiopia and Sinai and Jordan (after Johnson et al. 2011). Where, SM, Sahara Metacraton; CTB, Congo–Tanzania–Bangweulu Cratons; ZKC, Zimbabwe–Kalahari Cratons; I, Irumide Belt; A, Antogil Craton; M, Masora Craton; ANS, Arabian Nubian Shield. Capital names indicated here are not labelled on subsequent maps.

2.1.4 Geology of the Ethiopian basement rocks

The Ethiopian basement rocks are exposed in eastern, western, northern, and southern parts of the country (Fig. 2.4), (Asrat et al., 2001, Alene et al., 2000, 2006,).These rocks exposures are found in areas not intensively affected by Cenozoic volcanism and rifting and where the Phanerozoic cover rocks have been eroded away (Tefera et al., 1996). They have been

studied for the last decades by several researchers (Kazmin, 1971, 1975; Kazmin et al., 1978; Beyth, 1972; de Wit and Chewaka, 1981; Ayalew et al., 1990; Alemu, 1998; Tadesse, 1996; Teklay et al.,1998, Tadesse et al., 1997, 1999, 2000;Yibas et al., 2002,2000; Alene et al., 2000, 2006; Asrat et al., 2001,2004; Avigad et al.,2007).

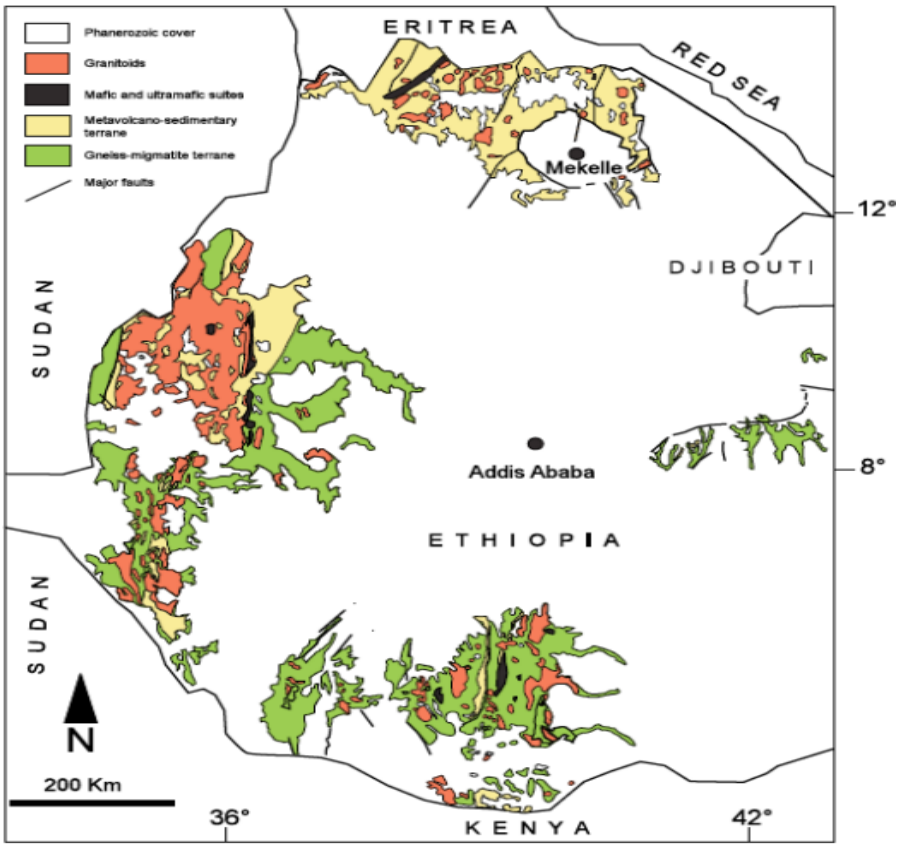

Figure 2.4 Exposure of the low grade volcano-sedimentary sequences of the ANS and high grade gneisses and migmatites of the Mozambique belt in Ethiopia (modified from Asrat et al., 2001, as cited in Solomon, 2009).

Kazmin(1971, 1975), have subdivided the basement rocks of Ethiopia in into Lower, Middle, and Upper Complexes based on compositional, deformational and metamorphic grade variations. Recently, this subdivision has been revised based on the geochronological and isotopic data (Teklay et al., 1998;Ayalew et al., 1990; Gerra, 2000), and the two distinct lithotectonic terranes classification which show contrasting lithological association, internal structures and grade of metamorphism (Yibas et al., 2000;Yibas, 2003), as (1) the granite-gneiss terrane, consisting of high-grade para- and ortho-gneisses and deformed and metamorphosed granitoids; includes, Lower and Middle Complex of (Kazmin,1971, 1975) old classification , and (2) the ophiolitic fold and thrust belts, consisting of low-grade, mafic–ultramafic and sedimentary assemblages

comprises all the rocks of the Upper Complex(Kazmin,1971, 1975).The Gneisic-migmatitic terrain, separated by numerous Ophiolitic sutures (Asrat et al.,2001).

2.1.5 Precambrian rocks of Northern Ethiopia

The northern Ethiopian Precambrian rocks are characterized by the occurrence of low-grade volcanic, volcano-sedimentary, mafic and ultramafic rocks of ophiolitic character, and plutonic rocks Beyth, (1972); Kazmin, (1972) and Mengesha et al., (1996). These rocks belong to the Arabian –Nubian Shield (ANS) sector of the East -African orogeny (Tadesse et al., 1999; Asrat et al., 2001).This terrain is dominantly characterized by steeply dipping and extensively folded, low-grade metamorphic rocks intruded by various granitic and mafic intrusions (Asrat, 1997; Tadesse, 1997; Alemu, 1998; Tadesse et al., 2000,). Beyth (1972) broadly subdivided the basement rocks of the ANS in the Tigray region into two groups based on stratigraphical relationships: (1) the Tsaliet Group, and (2) the Tambien Group. From the two groups the oldest being the meta-volcanic/meta-volcanoclastic unit (also called the Tsaliet Group), followed by phyllite, slate, and carbonate,which fall under the Tambien Group, and the syn- to post-tectonic plutonic units, granite to granodioritic composition (Tadesse et al., 2000; Asrat et al., 2001; Alene et al., 2006).

The nature of the contact between the Tsaliet and Tambien groups is controversial. Beyth (1972) recognized an unconformable contact, whereas Alene et al., (1998), describe aconformable, gradational contact.

2.1.5.1 Tsaliet Group

The Tsaliet group is well constrained in the Tigray region and covers most of the area of the region occupied by basement rocks (Fig.2.5). The Tsaliet Group are unconformably overlain by the metasediments of Tambien Group but the lower boundary is not exposed (Beyth,

1972). This group consists of calc-alkaline, island arc related metavolcano-sedimentary rocks including metavolcanic/volcanoclastic rocks, sericite-chlorite schist, slate, grey wacke, impure marble, calcareous siltstone, well bedded, intermediate to acidic welded tuffs, lappili tuff, agglomerates (Beyth,1972; Beyth et al.,2003,Tadesse et al.,1999; Alene, M.,1998;Alene et al.,2000,2006;).

Mineral assemblages in the Tsaliet metavolcanics indicate that peak regional metamorphism at pumpellyite–actinolite to lower green schist facies (Alene et.al., 2006).

2.1.5.2 Tambien Group

Tambien Group is mainly exposed in a series of synclinal inliers overlying the Tsaliet Group with gradational contact from west to east Maikenetal, Tsedia, Chehmit, and Negash (Alene et al., 2006, Garland, 1980). The Tambien Group of northern Ethiopia consists of an ~5-km-thick mixed carbonate siliciclastic succession (Swanson-Hysell, et al., 2015).

According to Beyth (1972) from the two major sequences in the basement of Tigrai, northern Ethiopia: the Tambien Group predominantly a metasediments in which two facies are distinguished: mai kenetal facies which is composed of four formation (Werii slate, Assem limestone, Tsedia slate and Mai kenetal limestone) and Negash facies composed of slate, quartzitic dolomite and limestone.

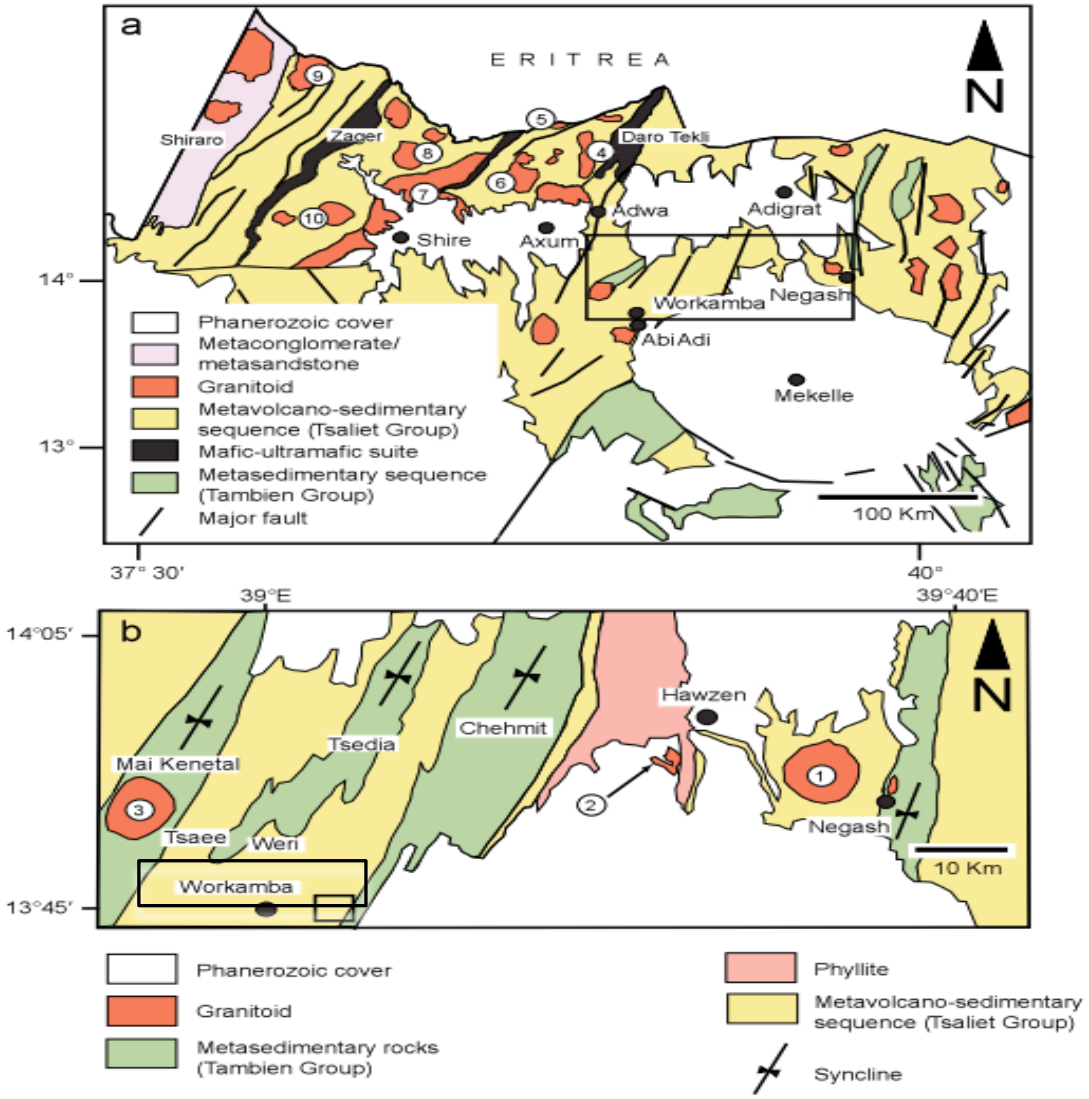

Figure 2.5 a) Distribution of the Tsaliet and Tambien groups in the Tigray region, northern Ethiopia. The inset great rectangle in (**f**igure 2.5 b) shows the study area where both Tsaliet and Tambien Group is exposed.(After Tadesse et al., 2000; Asrat et al., 2001; Alene et al., 2006,cited in Solomon, 2009). The circles with number represent the location of dated granitoids in the region, which are both syn- and post-tectonic in origin (1= Negash, 2 = Hawzen, 3 = Mai Kenetal, 4 = Rama, 5 = Mereb, 6 = Chila, 7 = Shire, 8 = Deset, 9 = Azeho, and 10 = Sibta granitoids).

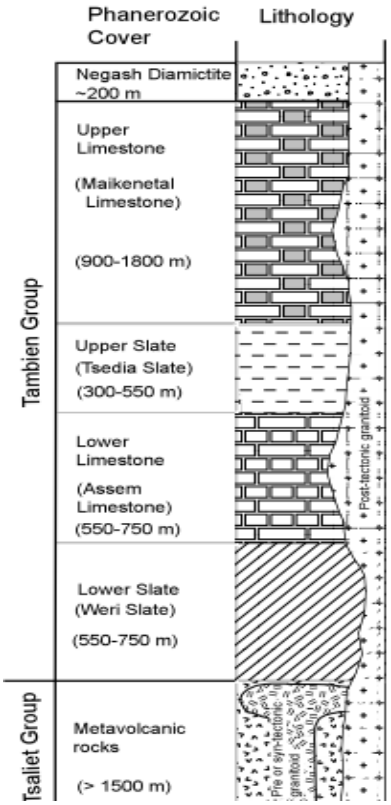

Figure 2.6 Stratigraphic sections of Tigray basement rocks showing relationship between the Tsaliet and Tambien group rocks. The pre- or syn-tectonic granitoids intruded the Tsaliet Group at about ~800 to 735 Ma, whereas the post-tectonic granitoids intruded both the Tambien and Tsaliet groups as well as the diamictites between ~620 and ~520Ma (after Beyth 1972;Alene et al., 2006;Avigad et al.,2007).

The Mai Kenetal synclinorium contains the most complete sequence of the Tambien Group rocks, which are from bottom to top (Fig.2.6): (i) the Lower Slate (Weri Slate), which mainly consists of black to blue-greenish, well laminated and foliated slate, greenish calcareous slate, and black silty greywacke.

Locally, this unit contains phyllite or graphite schist (Beyth 1972); (ii) the Lower Limestone (Assem Limestone) comprising mainly black to brown-greenish limestone (~90 wt. % calcite) with stromatolitic lamination and dark stylolites (Alene et al. 2006); (iii) the Upper Slate on top of the Lower Limestone consisting of purple silty non-calcareous slate, greenish grey feldspathic slate, greenish grey vitreous slate, and greenish grey slaty marl (Beyth 1972); (iv) the Upper Limestone, which is exposed at the core of the Mai Kenetal synclinorium. The Upper Limestone

is black in color and composed of up to 95 wt. % calcite with minor amounts of detrital quartz, and albite (Alene et al., 2006).

2.1.6 Regional Tectonic Setting

The basement rocks in north east Africa and Eastern Arabia is part of the ANS shield and represents predominantly juvenile continental crust that was formed differentiation of mantle largely without reworking of pre-existing continental crust (Stern, 1994; Stern, 2002; Johnson and Woldehaimanot, 2003).The major structural feature in the northern Ethiopia is the northeast-southwest striking and variably southeast and northwest dipping composite foliation (Tadesse, 1996). The tectonic structures recorded by the Tsaliet and Tambien group rocks are related to the collisional stress that resulted in the amalgamation of the ANS in Tigray and rocks have experienced different phases of deformations. Two phases of deformation (D1 and D2) are recognized by (Alene et al. 2006). Deformation D1 is caused by N-S compression and resulted in tight minor folds with a wavelength of several mm to dm, elongation lineation and pervasive regional foliation (Alene et al., 2006). D2 deformation resulted from E-W directed compression at the waning stage of the collision between East and West Gondwana and yielded long wave length (about 8 km), upright, open parallel folds without a significant cleavage, thrust, and strike slip faulting (Fig. 9., Alene et al., 2006). Major NE SW oriented synclinoria such as the Mai Kenetal, Tsedia, Chehmit and Negash, which folded the Tambien Group rocks are present in central Tigray (Beyth 1972; Alene et al., 2006).

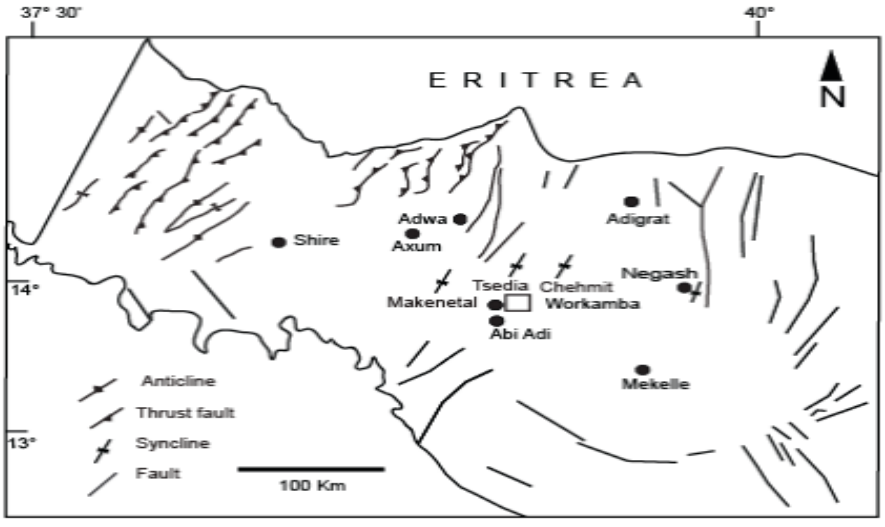

Figure 2.7 Distribution of major tectonic structures in Tigray (Tadesse, et al., 1996, 1999; Asrat, et al., 2001).

CHAPTER THREE

3. LOCAL GEOLOGYAND PETROGRAPHY

3.1 Introduction

The study area is part of the Precambrian rocks which constitutes both Tsaliet and Tembien groups. The Tsaliet group is represented by metavolcanics and volcaniclastic rock units which covers the most part of the study area (Fig.3.1). These rock units are overlain by metasediments of the Tembien Group which are represented by metalimestone, graphitic slate, phyllite and micaceous slate rock units and exposed in the North West and South-east of the mapped area. During the field work, lithologic units are described in terms of color, texture; mineralogy, metamorphism or alteration, degree of weathering and orientation of structural elements have been measured and described. The name for each lithological unit is given based on the textural and mineralogical constituent of the rocks observed during field study and both petrographic and geochemical analysis. In the study area nine mappable units are described (Fig.3.1) based on lithological composition and degree of deformation. Metavilcanic (MV) units cover most part of the study area and these include foliated metabasic (green-schist), nonfoliated metabasic, metabasaltic andesite with intercalation of tuffaceous layer, metavolcanoclastic and metabreccia rock unit whereas, metasedimentary rock units contains; phyllite unit, graphitic slate unit, micaceous slate unit and metalimestone unit. Most metavolcanic rocks of the study area are fine-grained metamorphosed basic to intermediate-acidic volcanic rocks with primary volcanic textures (porphyritic), and recognizable relict plagioclase.

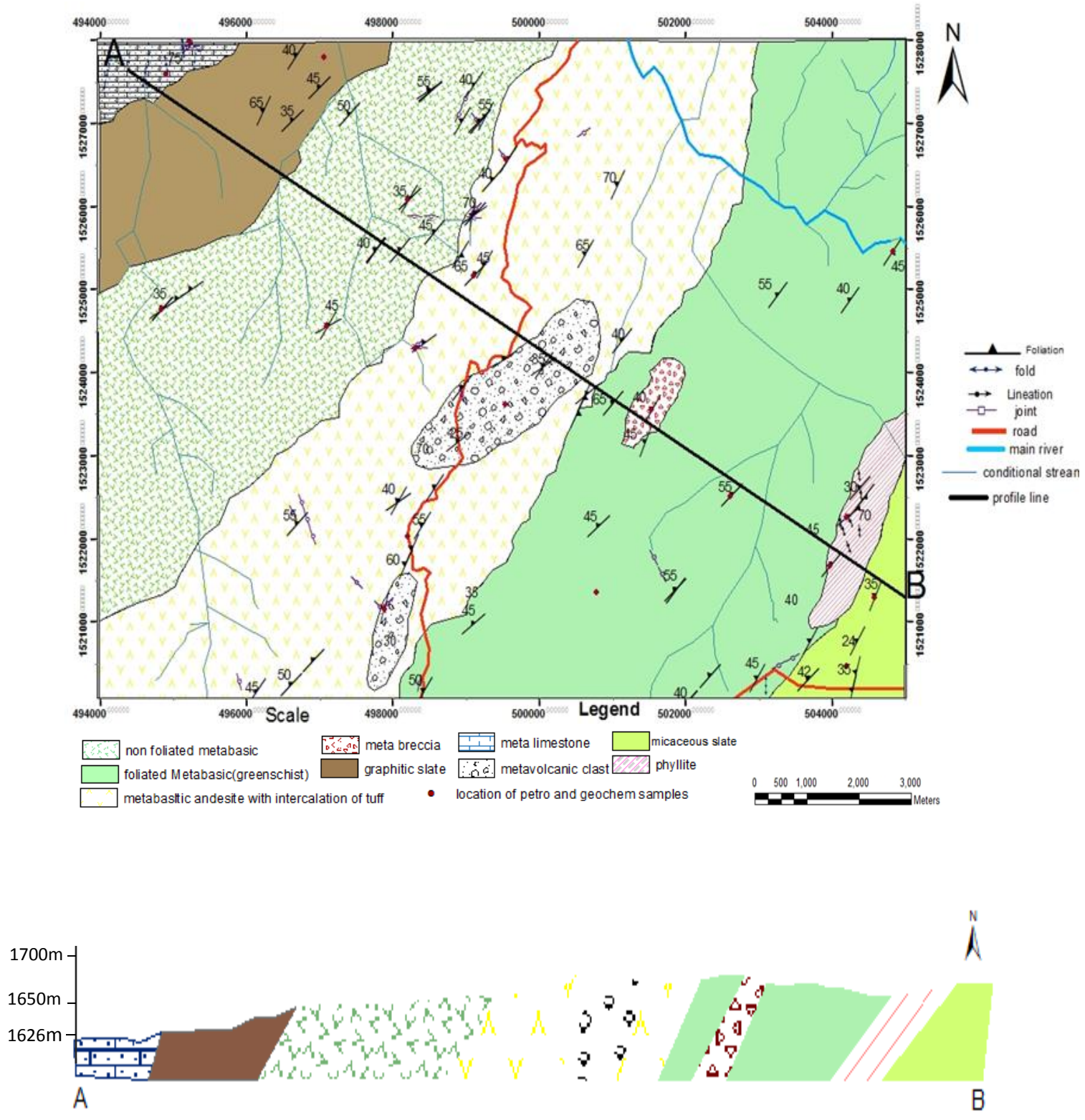

Figure 3.1 Geological map and cross section of the study area (Workamba area).

3.2 Foliated metabasic (greenschist) rock Unit

3.2.1 Field description

Foliated metabasic unit is exposed in the Eastern part of the mapped area (Fig. 3.1) and it has considerable broader area coverage compared to other lithological units. Texturally it is foliated and fine-medium grained. At places it shows well developed foliation with general trending $N20^0E$ to $N35^0E$ and dipping 45^0NW to 55^0NW. The out crop photo (Fig.3.2A) displys well developed foliation which can be define by fine grained weathered materials deflected around large massive fractured boulder. These structural features indicates that the rock has been well deformed.

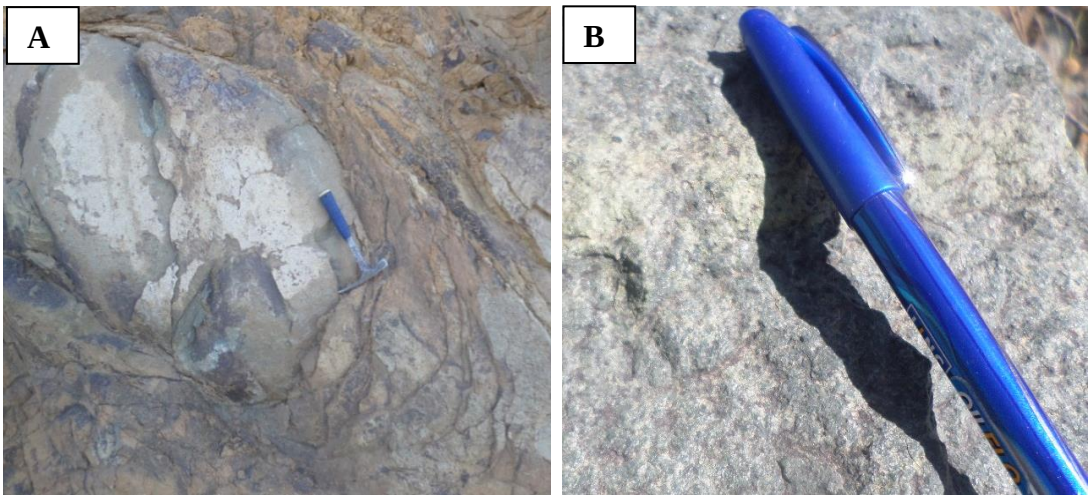

Figure 3.2 Field photographs of metabasic rock units which show foliated fabric nature of meta-basic. A) outcrop photo of meta- basic units in central south Eastern part of the study area (0502605E,1522515N, photo taken facing east) and B)outcrop photo of meta- basic rock unit from south east part of the study area (0498377E,152020N, photo taken facing west).

3.2.2 Petrography

Thin section study of representative samples from different locations (Fig.3.3 A-F) shows that the rock mainly consists of recrystallized quartz, epidote, chlorite, K-feldspar, plagioclase, mica, actinolite and opaque minerals. Significant amount of relict pyroxene and plagioclase are also visible. The characteristic mineral assemblage and alterations of these rocks are described from the following plates.

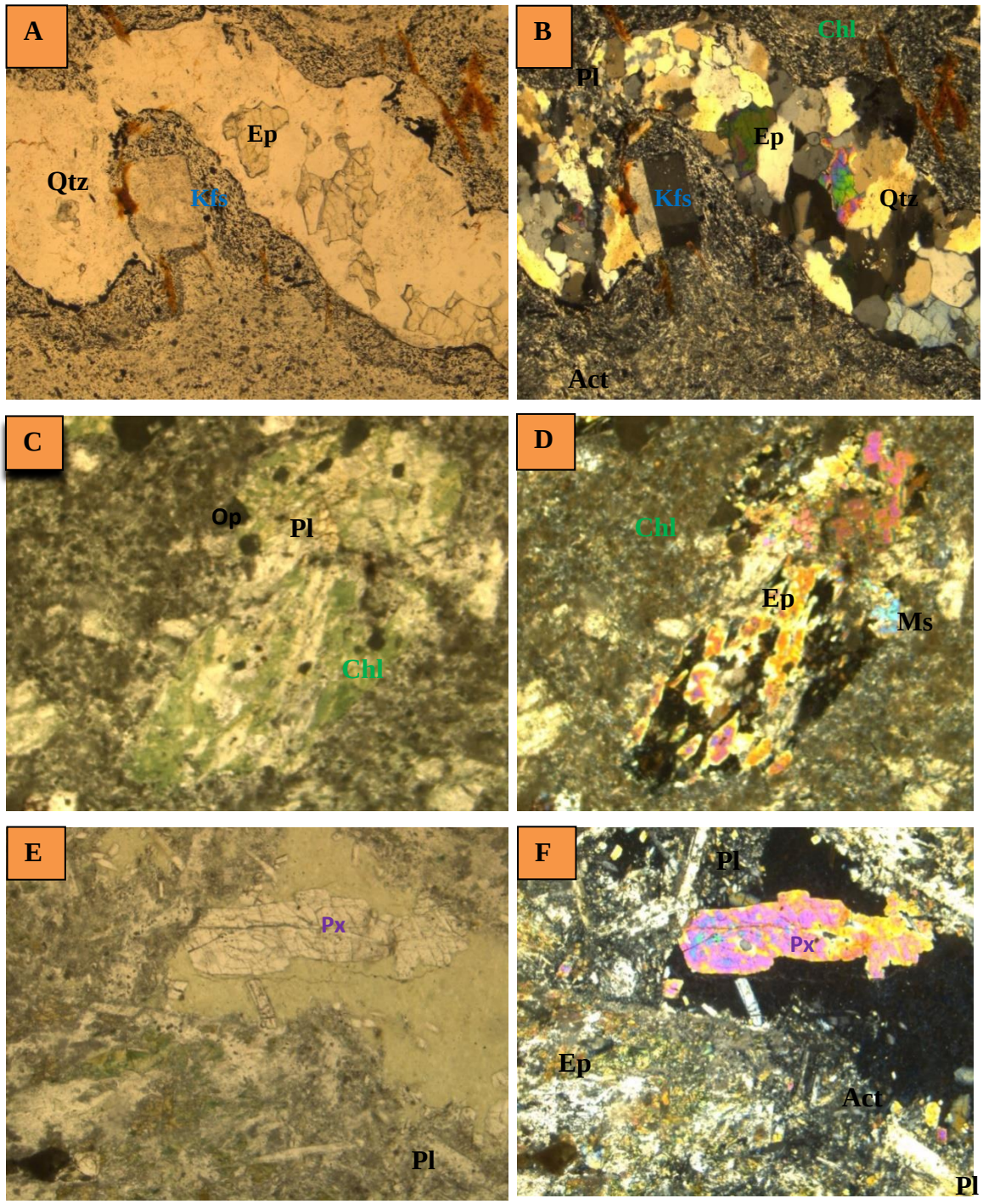

Figure 3.3 Microscopic photos of representative foliated metabasic with some relicts of K-feldspar and pyroxene under PPL and XPL with (40x magnification) from different locations. Plate A and B, are the same samples (W1) where A is in PPL but B in XPL, at sample location of (0498377E, 152020N), plate C and D are in PPL and XPL view respectively from sample (W16) at location of (0502605E, 1522515N) and plate E in PPL and F in XPL view from sample (W19) at location of (0504927E, 1525627N).

Plate A and B has an average mineral content of; chlorite, 40%, quartz 5%, actinolite 15%, epidote 15%, plagioclase15%, K-feldspar 5%, and opaque minerals 5%. The above photographs (A and B) shows porphyroclast of k-feldspar is enveloped by deformed layer of fine grained chlorite schist and recrystallized quartz grains with epidotization. These mineral assemblages and schistosity development used to evaluate the relationships between metamorphism and deformation. Plate C and D contains mineral content: chlorite 40%, epidote 25%, plagioclase 20%, mica 10%, and opaque minerals 5%. Petrographic analysis shows that Ca-rich plagioclase is altered to Na-rich plagioclase.

Another thin section analysis under plate E and F reveals that the mineral content of: chlorite 40%, plagioclase 25%, epidote 15%, relic of pyroxene 15%, actinolite 5%. In (photo E and F) the pinkish color under XPL and gray color under PPL indicates the relic of pyroxene.

3.3 Nonfoliated metabasic rock unit

3.3.1 Field description

This rock unit occurs in the Western part of the study area (Fig.3.1). The unit forms a rugged topography and it varies in width along the strike of the layering that it is wider in the South and narrower in the North. The rock varies from black to light grey and shows, nonfoliated/massive course grained texture and contains plagioclase crystal up to 2cm in length.

3.3.2 Petrography

The petrography analysis from representative rock thin sections (Fig.3.4 A and B) shows that the mineral content includes: plagioclase 65%, epidote 15%, quartz 5%, relic of pyroxene 10%, and opaque minrals 5%. Therefore the presence epidote, sodic plagioclase, quartz and relict pyroxene indicate that the rock unit has been subjected to low grade (green schist facies) metamorphism. Generally the mineral assemblages suggesting that they are typical metamorphosed products of mafic to intermediate volcanic rocks.

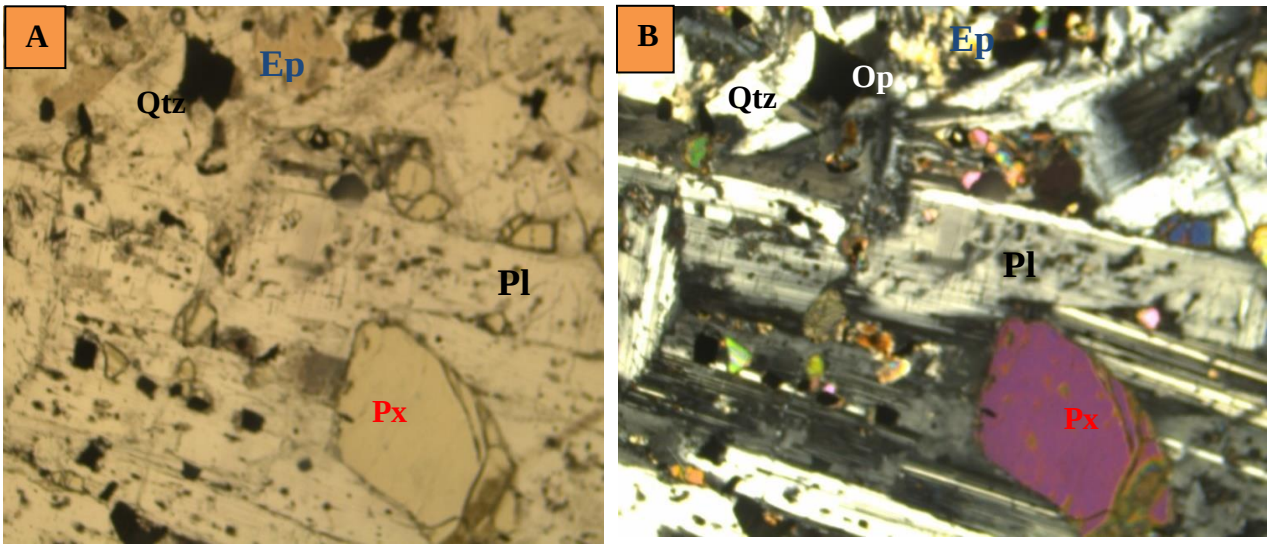

Figure 3.4 Microscopic photos of nonfoliated metabasic with relict pyroxene under PPL and XPL view (40 x magnifications) from different locations. Plates (Fig.3.4 A and B) are thin section of representative rock samples (W7) which is at location of (0494830E, 1524760N). Thin section (A&B) has euhedral pyroxene phenocryst as inclusion within an elongated plagioclase and XPL view (B) shows slightly altered relict plagioclase.

3.4 Meta-breccia rock unit

3.4.1 Field description

This unit has small area coverage compared to other mappable units and is found in the eastern part of the study area within meta-basaltic unit. The rock has a foliated fabric, it contains large, angular, 15-50cm clasts and it is brownish to gray color (Fig.3.5A and B). At the hand spacemen the rock is hard and contains random oriented angular clasts of mafic to intermediate composition. Locally it shows a trend of $N20^0E$ to $N30^0E$ and 40 to 55 dipping towards NW.

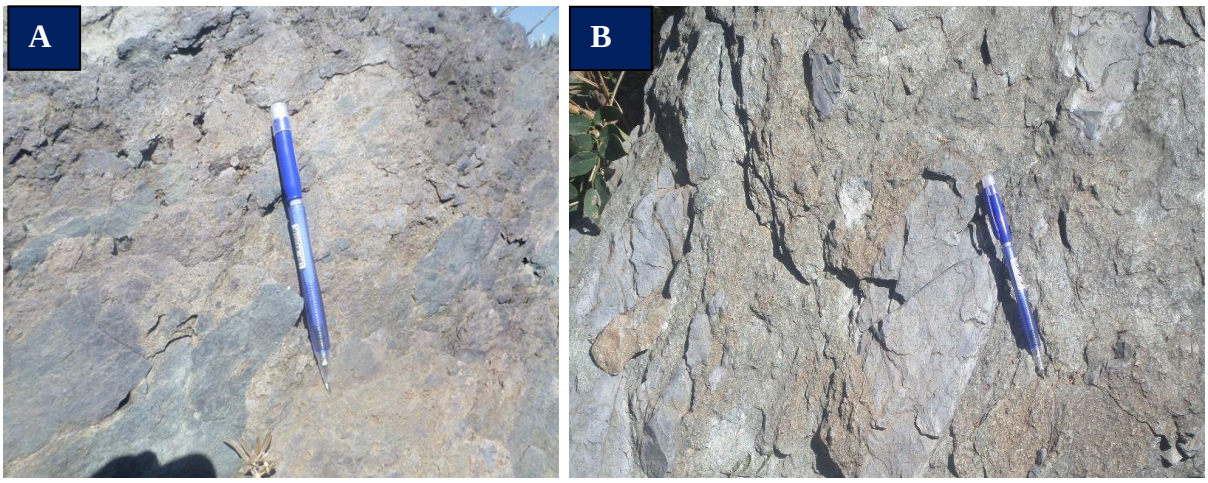

Figure 3.5 Field photographs of metabreccia which reveals angular to sub angular clasts A) Elongated, large (>5cm) mafic clasts (location: 0501529E, 1523555N) photo taken facing west B). metabreccia rock unit at location of (0502004E, 1520019N) displaying grey, angular clasts, and photo taken facing east.

3.4.2 Petrography

Thin section investigation of representative sample (Fig.3.6A and B) shows that the unit is mainly composed of quartz, calcite, and muscovite, fine-grained maficand opaque minerals. Elongated angular clasts are compacted by fine-grained mafic matrix. Elongated quartz and calcite grains are observed parallel to the main foliation (Fig.3.6 A and B). Its average modal composition is quartz 45-50%, calcite 20-25%, muscovite 10-15%, and opaque minerals 5-10%.

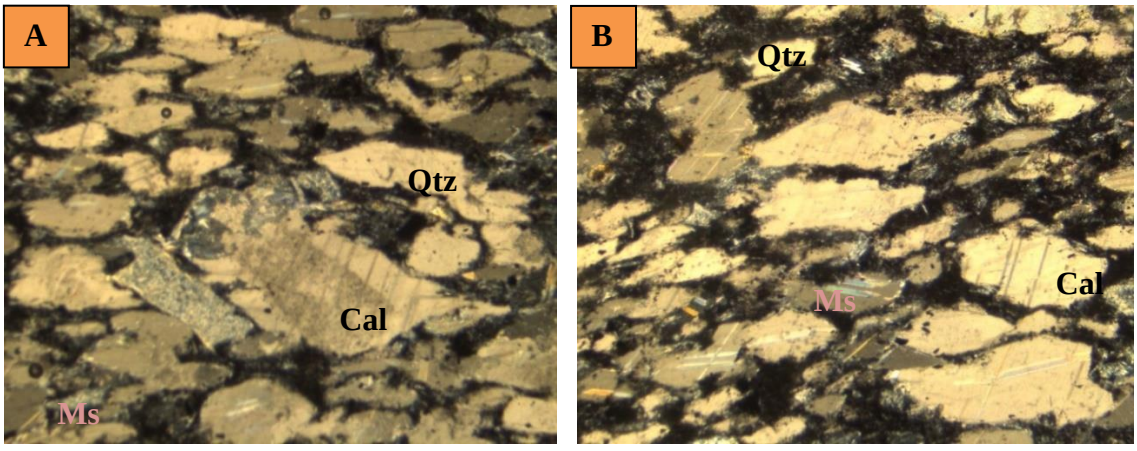

Figure 3.6 Microphotographs of metabreccia with elongated clasts of calcite and quartz for sample (W15) with different field of view with l(40x magnifications) and the sample was taken at location of (0501529E, 1523555N).

3.5 Meta-volcanic clast rock unit

3.5.1 Field description

This lithological unit is exposed mainly in the central part of the mapped area (Fig.3.1) and it is found intercalated with the other units. It characterized by the occurrence of sub-rounded to rounded black to grayish volcanic clasts within fine to medium grained matrix. The clast size is variable throughout the unit and it ranges from 10 - 45 cm. The size of clast is nearly similar with that of metabreccia rock unit which described in (Fig.3.5 and 3.6) but, their mineralogy and shape is different. From field observation and petrographic analysis the meta-volcanic clast shows round to sub rounded clast shape but meta-breccia reveals angular clasts. The nature of exposer is discontinuous through mapped area (see Fig.3.1) and it shows general trend NE and dipping towards North West. This lithologic unit is also characterized by undulating topographic features.

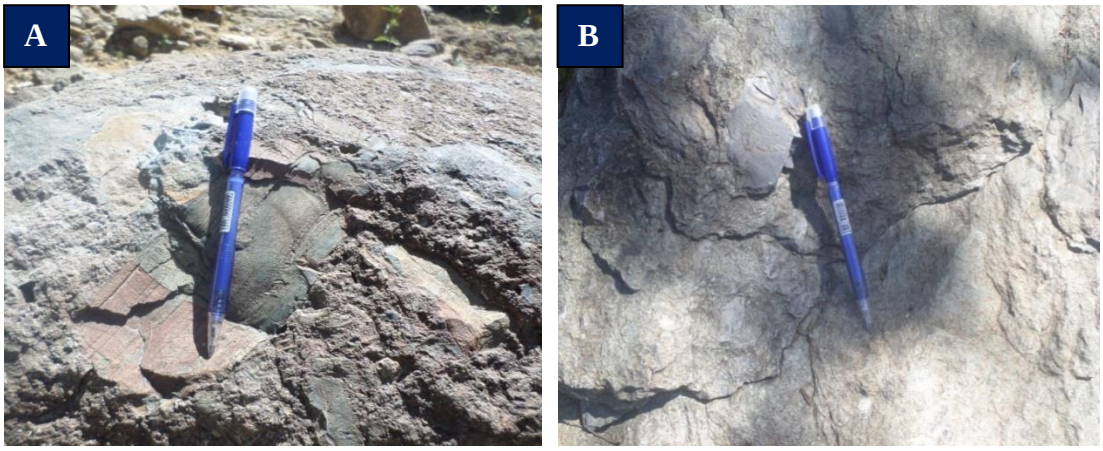

Figure 3.7 Field photos which displays large meta-volcanic clasts surrounded within fine-grained matrix A) photo of metavolcanic clast unit from southern part of mapped area (0498160E,1522175N, photo taken facing north) B) photo of metavolcanic clast unit from central part of mapped area (0498870E,1523159N, photo taken facing west).

3.5.2 Petrography

Petrographic analysis (Fig.3.8 A and B) shows random distribution of large fragments of quartz and altered plagioclase with fine grain mafic minerals. The unit is mainly composed of quartz, altered plagioclase, chlorite, epidote and opaque minerals. The large clasts are being wrapped by the mica minerals with weakly developed schistosity. Recognizing the relationships between the

clast and external foliation is used to suggest deformation-metamorphism interrelationships. The average modal composition is quartz 35-40%, plagioclase 15-20%, chlorite 10-15%, epidote 5 - 10%, altered muscovite 5-10%, and opaque mineral 5%. Plate B shows that fine grain chlorite enveloped the fragmented quartz and altered plagioclase and the alteration of mafic minerals as revealed by development of epidote.

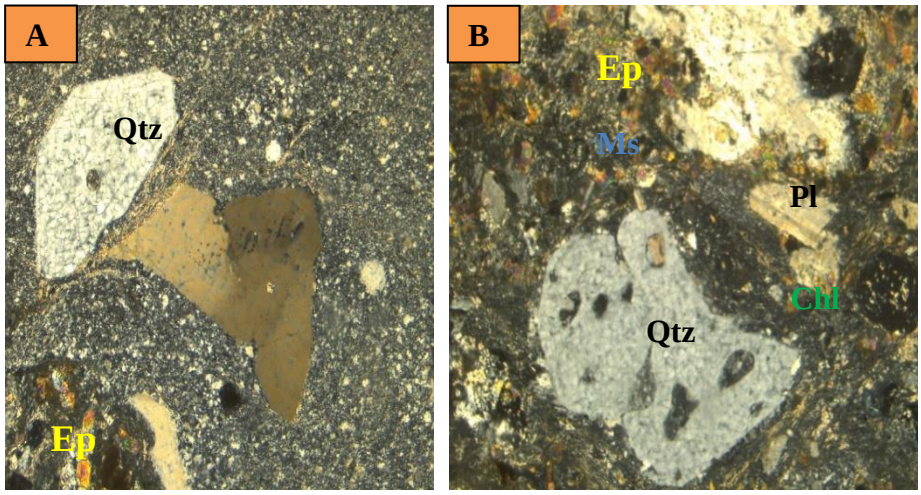

Figure 3.8 Microphotographs of sub rounded metavolcanic clasts under XPL with different field of view (40x magnifications). Both are from the sample (W2) and the sample taken at location of (0498160E, 1522175N). In plate A the large sub rounded clasts are found within fine to medium grain of glassy and mafic mineral matrix, whereas Plate B displays that relatively small clasts are engulfed within subrounded quartz fragment and foliation is welldeveloped in the by enclosing the quartz fragment.

3.6 Metabasaltic-andesite with intercalation of Tuffaceous layer

3.6.1 Field description

Metabasaltic-andesite unit with intercalation of tuffaceous layer is exposed in the central part of mapped area (Fig.3.1).The unit shows some textural and compositional variation across the study area. In this unit metabasaltic-andesite rock is characterized by greenish to light grey fresh color with massive medium to course grained foliated texture and it consisting of relict of quartz and feldspar grains. At hand specimen, petrographic and geochemical description compositionally it varies from metabasaltic-andesite to felsic. Even though this rock unit strongly foliated, original tuffaceous layer is common in some part of mapped area. At some places foliated tuff is highly

weathered and display light brownish color. It differs from the above mentioned metabasic by its composition.

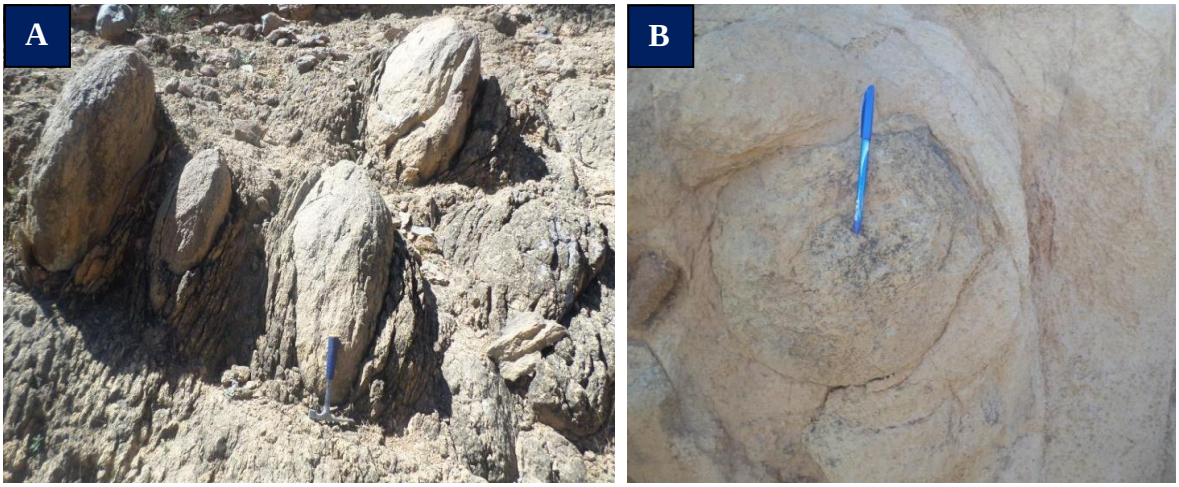

Figure 3.9 Field photos of metabasaltic-andesite which reveal well developed foliation A) out crop photo of metabasaltic-andesite from central part of mapped area (0499173E, 1526998N, photo taken facing south) B) photo of meta-andesite with deformed texture at location (0498297E,1524287N, photo taken facing north).

3.6.2 Petrography

Thin section study of metabasaltic-andesite of representative samples (Fig.3.10A-J) shows that slightly developed foliation and some igneous relicts are randomly distributed within fine grain matrix. The unit is mainly composed of plagioclase, epidote, k-feldspar, chlorite, quartz and muscovite with significance amount of actinolite/tremolite. From petrographic analysis the relationship between igneous relicts with external foliation used to evaluate metamorphism and deformation history of the area because, large scale geologic events are recorded in microscopic level.

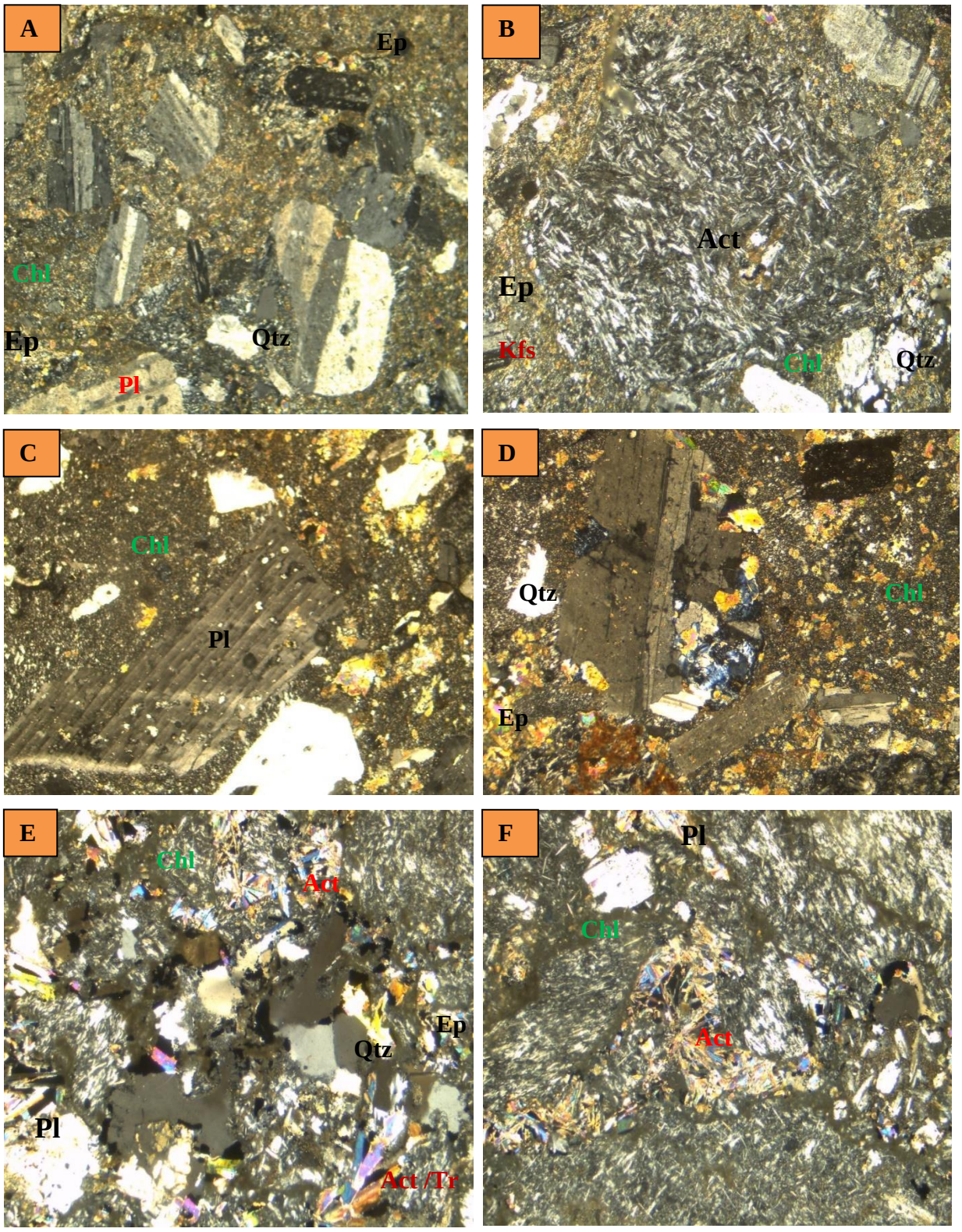
A
Ep
Chl
Ep
Qtz
Pl
B
Act
Ep
Kfs
Chl
Qtz
C
Chl
Pl
D
Qtz
Chl
Ep
E
Chl
Act
Ep
Qtz
Pl
Act /Tr
F
Pl
Chl
Act

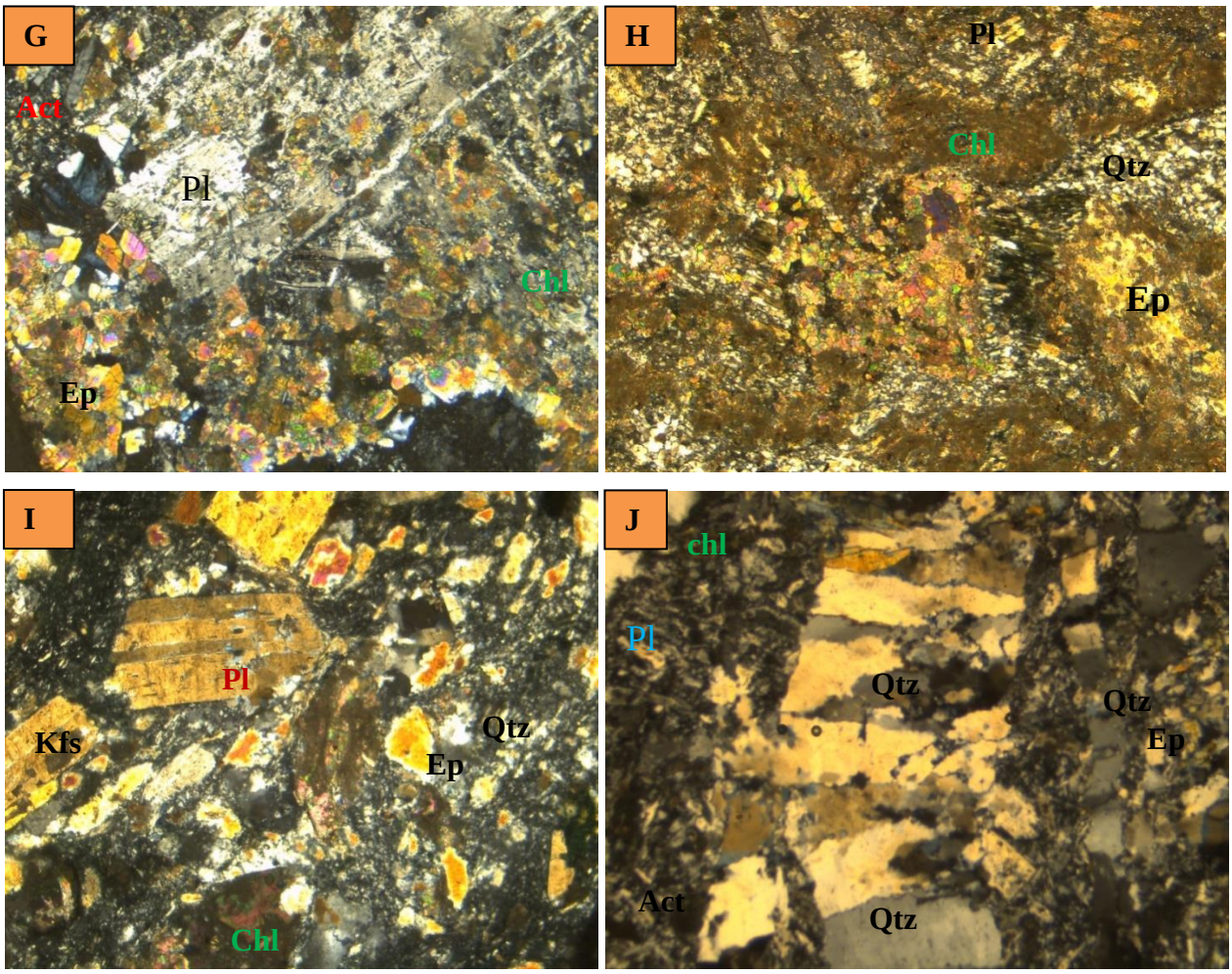

Figure 3.10 Microphotographs which are representative of metabasaltic-andesite from different location and all are under XPL view with (40x magnifications). Plate A and B are the same sample (W13), at sample location of (0498297E, 1524287N), Plate C and D are for samples (W5) at location (0499108E, 1525170N), Plate E and F are the same samples (W6) with different field of view and the sample taken at location of (0497089E, 1524560N), plate G for metabasalt (W4) at location of (04960187E, 1520081N), Plate H is for sample (W14), at location (0499551E, 1526567N), Plate I from sample (W3) in metabasalic-andesite that has been taken at location of (0497877E, 1521154N), and another plate J represents sample (W9), at location of (04950165E,1526226N).

In plate A is an altered relict of k-feldspar is irregularly distributed in fine grain matrix whereas, thin section B reveals trachytic texture phenocryst bounded by microcrystalline matrix of epidote and chlorite. Within phenocryst hair like white actinolite minerals shows preferred alignment in specific direction.

Plate C and D have an average modal composition of chlorite 30%, relict of k-feldspar 25%, actinolite 20%, plagioclase 10%, epidote 5%, and quartz 5% with rare amount of opaque minerals. These plates show weak foliation and contain chlorite 35%, epidote 33%, plagioclase, 25%, and quartz 7%. Under plate C plagioclase shows undulose extinction and that indicates the rock has been subjected to some deformation. Plate D displays plagioclase alteration and epidote over growth as inclusion.

Plate E and F consists of actinolite 40%, plagioclase 25%, quartz 6%, chlorite 15%, epidote 10% and opaque mineral 4%.These plates characterized by suture boundary and preferred orientation of medium to coarse grain minerals which reflect its degree of foliation.

Thin section G shows altered plagioclase and it mainly contains epidote 35%, altered plagioclase 30%, chlorite 20%, actinolite 5%, and quartz 5%.

Plate H shows suture (zigzag) boundary between chlorite and fine grain quartz, and that results from later deformation. Its mineralogical constitute is chlorite 40%, epidote 35%, quartz 5%, plagioclase 15% and opaque mineral 5%. It also characterized by fine grain foliated texture.

Plate I shows relict of k-feldspar which is bounded by fine to medium grain of epidote, chlorite and quartz and it characterized by slightly foliated texture. The relict of k-feldspar in (Fig.3.10 I) characterized by its simple twining.This plate mainly composed of: chlorite 35%, plagioclase 25%, epidote 20%, quartz 15% and opaque mineral5%.

Plate J contains an average mineral content of plagioclase 30%, actinolite 20%, chlorite 15%, recrystallized quartz 10%, epidote 3%, and opaque minerals 2%. In this plate quart shows undulose extinction and indicates that after quartz grain formed it was subjected to deformation.

3.7 Phyllite rock unit

3.7.1 Field description

The phyllite rock unit is exposed in south eastern part of mapped area (Fig.3.1). This unit is found in between the metavolcanic and micaceous slate units and it shows gradational contact with both units. The characteristic color of this unit is light grey with fabric-forming mica minerals which show shiny surfaces. It is characterized by that all part of the unit is highly foliated and crenulated texture and the foliation is mainly striking NE direction with dipping 30-40 NW. This rock unit lies on flat topography relative to the whole mapped area and quartz veins are common across the foliation direction.

3.7.2 Petrography

Petrographic analysis shows that the unit is mainly composed of muscovite/sericite, chlorite, quartz, epidote and opaque minerals (Fig.3.11). The foliation is displayed by preferred alignment of minerals and concordant with compositional layering. Figures 3.11 A and B show crenulation cleavage and that indicate the rock has been subjected to at least phases of deformation. It also shows well developed schistosity which displays by preferred alignment of platy minerals.

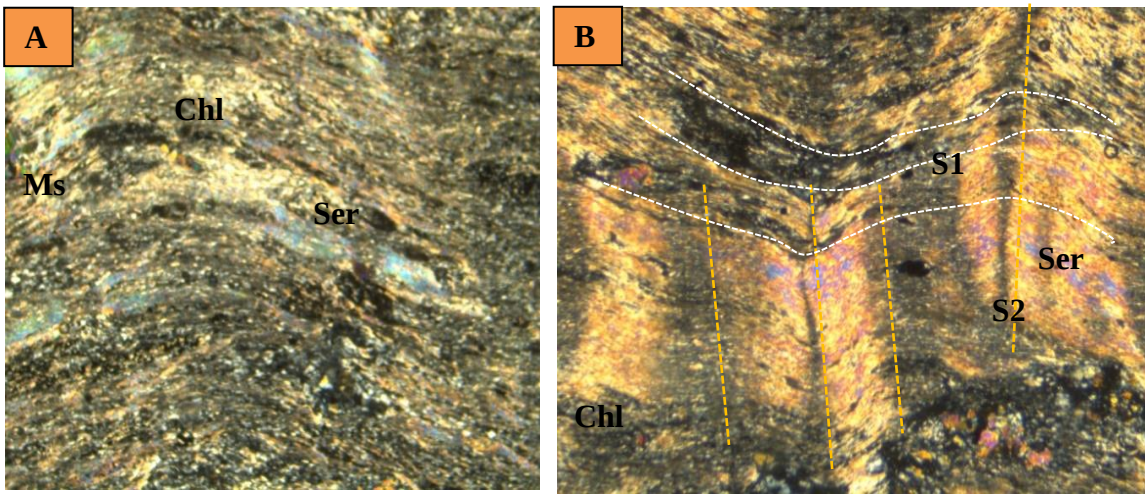

Figure 3.11 Microphotographs of phyllite which reveal crenulation cleavage. Both are for sample (W20) at location (0503971E, 1521677N) under XPL view with (40x magnification).

Plate A and B reveals well developed S1foliations and S2 crenulation cleavage. In plate B S1foliation is well developed horizontally but, S2 foliation is display vertical to S1 foliation. These microstructural features indicate that S0 is affected by S1foliation and S2 is developed by D2 deformation. It consists of mineral content of muscovite/sericite 60%, quartz 20%, chlorite15%, and opaque 5%. Generally from petrographic study in plate A and B the existence of minerals (chlorite and quartz) with field observation suggests that the phyillite unit have volcanic origin.

3.8 Micaceous slate rock Unit

3.8.1 Field description

Slate unit is exposed in south eastern part of the mapped area (Fig.3.1).The unit is characterized by fine grained texture and light grey color with slaty cleavage. It shows gradational contact relationship with the adjacent phyllite unit. From the field observations (Fig.5.1B) it shows that

compositional banding and cleavage are parallel to the regional foliations. It forms gentle topography with the adjacent phyllite rock unit relative to other map able units.

3.8.2 Petrography

Thin section study (Fig.12A and B) from slate unit displays that the rock dominantly composed of mica 65%, quartz 20%, epidote10% and opaque minerals 5%. It also reveals brownish to grey color and fine grained texture. Slightly developed crenulation is display by small scale folded structure of mica.

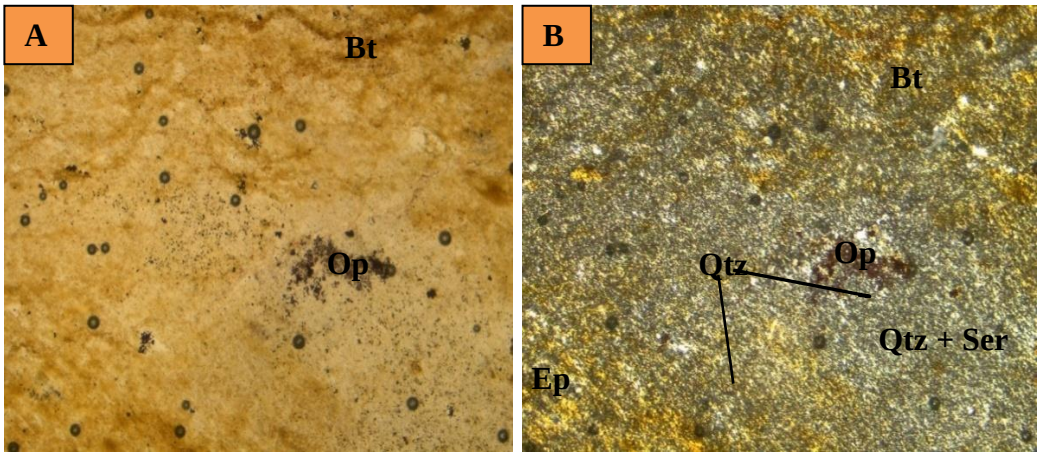

Figure 3.12 Microphotographs of slate under PPL and XPL view with (40x magnifications). Plate A and B are the same sample (W20) which has been taken at location of (0503740E, 1520250N).

3.9 Graphitic Slate rock Unit

3.8.1 Field description

Graphitic slate unit is exposed in north western part of the mapped area (Fig.3.1).The characteristical color of the unit varies from light grey, grey-green to purplish as shown in (Fig.3.13A) with compositional layering.The unit has fine grain well foliated texture with slaty cleavages that are parallel to the regional foliations and it affected by joints (Fig.3.13B).

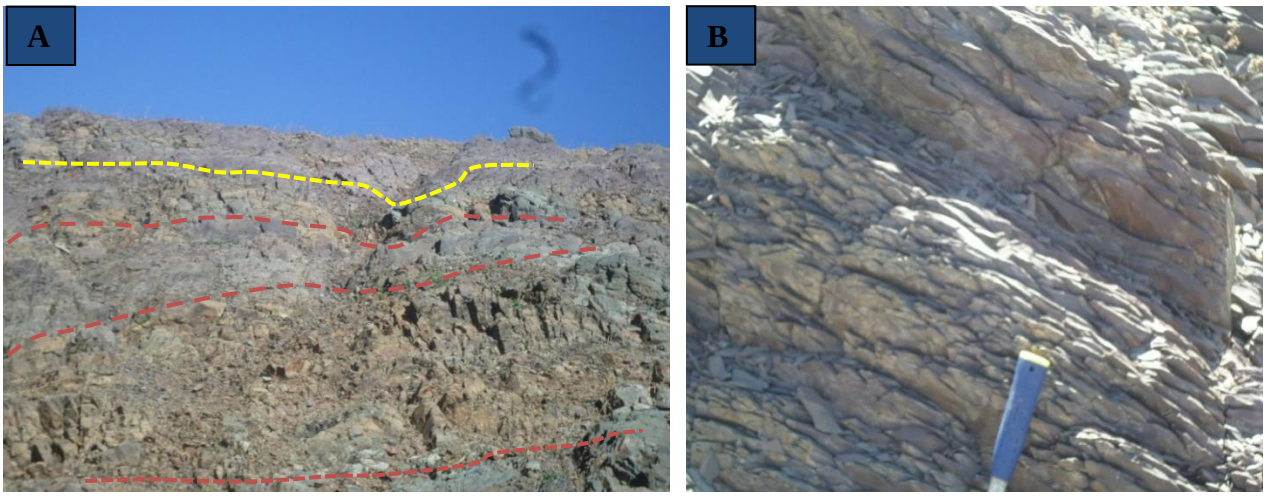

Figure 3.13 Field photographs of graphitic slate unit with compositional layering and slaty cleavage, A) out crop photo graphitic slate unit from western part of mapped area (0497053E, 1527806N), photo taken facing north and it shows compositional layering B)out crop photo of pencil like graphitic slate from (0496601E,1527026N) photo taken facing north and it displays slaty cleavage.

3.8.2 Petrography

Thin section study of graphitic slate (Fig.3.14A and B) indicates that average modal composition is graphite 35%, mica 30%, quartz 25% and opaque minerals 10%. In (Fig.3.14A) compositional banding between graphite and felsic minerals shows weakly developed primary foliation.

Foliation is displayed by directional alignment of micacceous minerals (Fig.3.14B). These fine grained minerals reflect that the rock has been subjected to very low grade metamorphism.

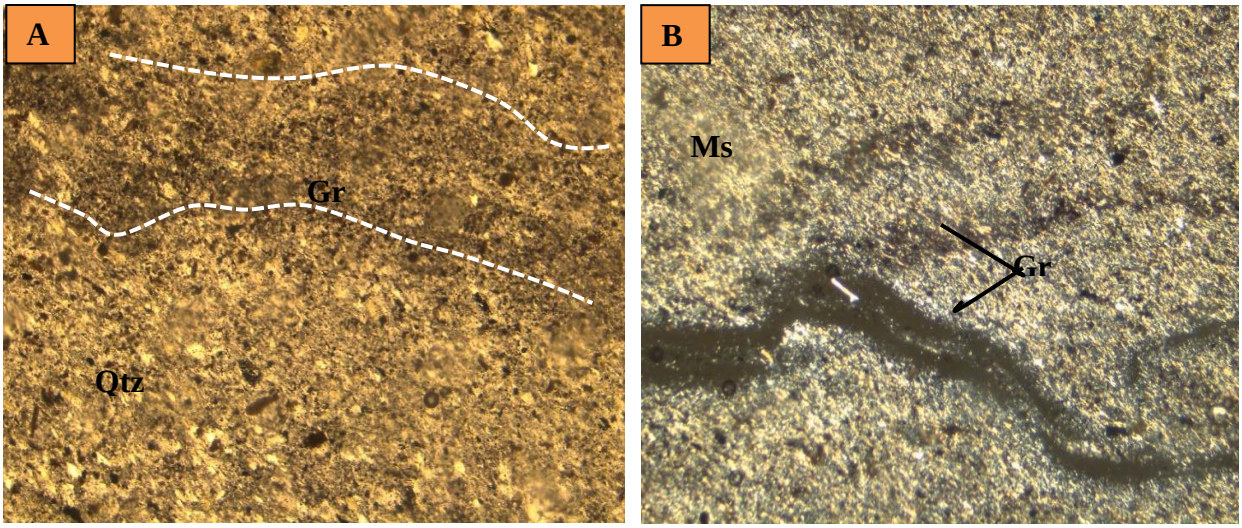

Figure 3.14 Microphotographs of graphitic slate under XPL view with different field of view (40x magnifications). Plate A and B represents the same sample (W10) for graphitic slate (0497053E,

1527803N) with different field of view. Thin section A under XPL view shows compositional banding whereas plate B indicates micro fold of dark color graphite with fine grain micas S1foliation.

3.9 Metalimestone rock unit

3.9.1 Field description

Metalimestone unit is found northwestern part of the study area (Fig.3.1) and it conformably overlies the graphitic slate. The unit is characterized by highly laminated and folded structures and has fine grained massive texture with grey to black color. It is exposed over 60m thick section and is affected by different set of joints (Fig.3.15).

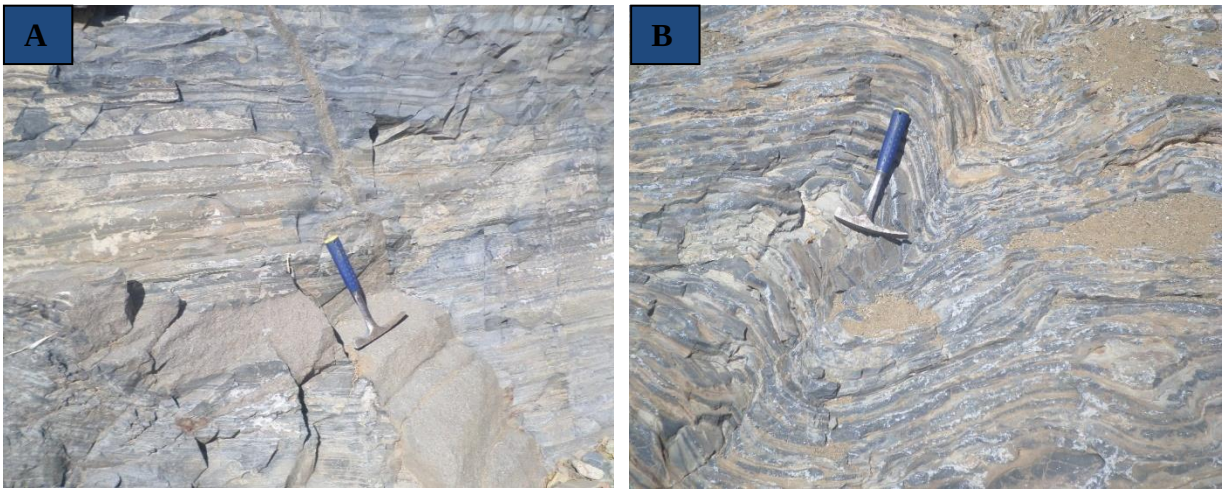

Figure 3.15 Field photographs of metalimestone, A)outcrop photo from western part of the study area (0495213E,1527991N) photo taken facing west and the joint is filled by mica mineral B) outcrop photo from western part of the study area at location of (0495206E,1527989N) photo taken facing west that reveals folded structure.

3.9.2 Petrography

Thin section study of metalimestone (Fig.3.16 A -D) reveals that the rock mainly composed of fine grain calcite with thin laminated clay minerals. The unit is characterized by mica filled vein and clay rich layers. Mica rich vein is discordant to compositional banding of calcite and clay rich layer (Fig.3.16A and B). Another representative thin section (Fig.3.16 C and D) reveals that primary lamination is distinguished by compositional layering between calcite rich and clay rich fabric.

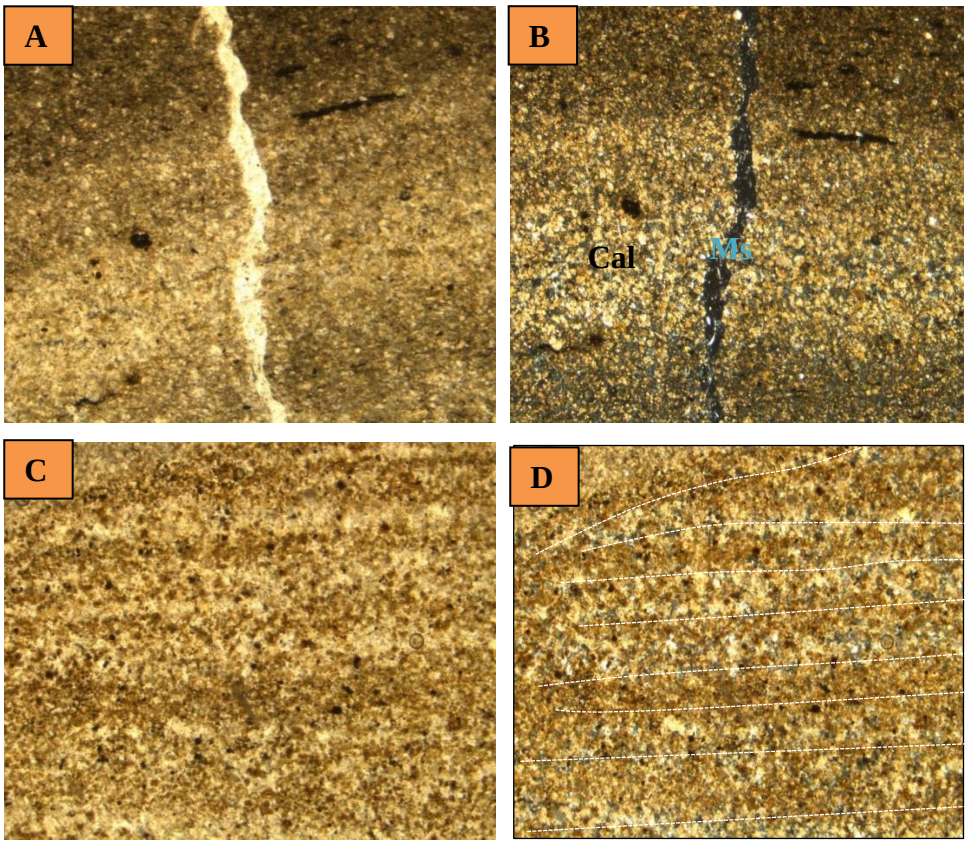

Figure 3.16 Microphotographs which displays lamination of metalimestone for sample # W12(A and B) and sample # W11 (C and D) under PPL and XPL view with (40x magnifications) where, location of samples are (0495206E, 1527989N) and (0495213E, 1527991N) respectively.

Plate A and B represents mica filled vein of metalimestone rock unit that shows the rock has been affected by some deformation and fracture is developed vertical to primary bedding. The average mineral content of this plate is calcite 70%, mica 20%, clay mineral 12% and opaque mineral 3%.Plate C and D are the same sample under PPL and XPL view respectively. The mineral content: calcite 75%, mica 15%, clay 10%.It shows compositional banding between light color calcite and clay rich dark grey colored layers.

CHAPTER FOUR

4. METAMORPHISM OF METAVOLCANICS

4.1 Introduction

Petrographic analysis has been conducted on twenty one thin sections that representing all major lithological units of the study area. From field observation and thin section analysis these rocks have experienced a change in mineralogy. Identification of index mineral assemblage, visually estimated modal abundance of constituting minerals, the presence of relict mineral and mineral alterations is used to evaluate the grade of metamorphism and metamorphic facies. From thin section study of representative rock samples the presence of recrystallized quartz, altered feldspar, and secondary minerals such as epidote, chlorite, actinolite, sericite, muscovite, calcite, graphite and porphyroblasts of opaque minerals indicate significant mineralogical change during metamorphism. Therefore the above benchmarks indicate that the study area undergo regionally low grade metamorphism.

Some rocks have preserved their original relict minerals and these features are used to determine protolith (the parent rock). Analyzing to what extent the original structures and textures of the parent rocks are preserved in the rocks also enable us to understand the history of metamorphism.

4.2 Metamorphism of the metavolcanic rock units

The metavolcanic rocks of the study area are fine-grained metamorphosed basic to intermediate-acidic volcanic rocks with primary volcanic textures (porphyritics) and recognizable igneous relicts. Therefore, the mineral assemblages of metavolcanic rocks which found in the study area are characterized by the existence of relict of plagioclase, olivine, pyroxene and k-feldspar phenocrysts, with metamorphic minerals such as epidote, chlorite, muscovite, calcite, tremolite/actinolite, quartz and opaque (Fig.3.3A and E).This mineral assemblage and the revealed textures are indicative features of green-schist facies that results from low grade metamorphism of originally volcanic rocks. In most metavolcanic rock thin sections chlorite is modally abundant mineral is probably derived from mafic minerals in the matrix. Epidote is also common abundant mineral in meta-basaltic andesite rocks of the study area and occurs as

medium to coarse grained mineral in the matrix. Epidotization in metavolcanic rock depicts that alteration of ferromagnesian minerals.

4.2 Metamorphism of the metasedimentary rock units

Petrographic analysis of metasedimentary rocks of the study area shows that it mainly composed of chlorite, muscovite/sericite, quartz, graphite, calcite, biotite and opaque.

The above mineral assemblage indicates that clearly these rocks are subjected to low grade metamorphism. Chlorite and muscovite are the more abundant minerals in the phyllite and slate rocks and these are probably recrystallized from clay minerals such as illite, kaolinite and montimorinolites indicating low grade metamorphism of shale or mudstone.

In graphitic slate and metalimestone (Fig.3.14 and 3.16) primary bedding is visible and that reveals the protolith was sedimentary rocks. The above mentioned mineral assemblage with preservation of primary structures indicates that the rock has been subjected to low grade of metamorphism (green schist facies).

The most dominant critical mineral assemblages of the various rock units are shown below. The critical minerals that used to evaluate the grade of metamorphism/facies are in bold and underlined.

1. Foliated metabasic
    a) **Chl**+ **Ep** +**Act** + Qtz + Pl+Op
    b) **Chl** + **Ep** + Qtz + Pl + Ms +Op
    c) **Chl** +**Ep** + **Act** +Pl +Px
2. Non foliated metabasic
    a) **Ep** + Pl + Qtz + Px + Op
    b) **Ep** +Pl +Qtz + Op
3. Meta-breccia
    a) **Ms** + Cal + **Chl** + Qtz +Op
4. Metavolcanic clast
    a) **Chl** + **Ep** +MsQtz + Pl + Op
5. metabasaltic-andesite
    a) **Ep**+**Chl** + **Act** +Pl + Qtz
    b) **Ep**+**Chl**+ Qtz+Pl +Op

c) **Chl** + **Ep** + Pl + Qtz + Op

6. Phyllite

a) **Ms/Ser** + **chl** +Ep+ qtz + Op

b) **Ms/Ser**+ **chl** + qtz + op

7. Micaceous slate

a) **Ms/Ser** + **Chl** + Qtz+ Op

8. Graphitic slate

a) **Ms**+ Gr + qtz + Op

9. Metalimestone

a) Ms+Cal + Qtz+ Op

b) Ms +Cal + Qtz

The main possible metamorphic mineral reactions for metamorphic rocks of the study area is predicted from rock composition and its mineral assemblage associate with dominant alteration (chloritization, sericitization, actinolitization, carbonization and oxidation) which is producing secondary minerals such as chlorite, sericite, actinolite and calcite.

For example, Chlorite + Epidote = Plagioclase + Qtz + Mg-richer Chlorite + Water

Epidote + Actinolite + CO_2 = Calcite + Chlorite

In generally these mineral asseblages reveal that all of the studied rocks have been underwent regional metamorphism in the lower green schist facies. Regionally the Tsaliet group metamorphic rocks in northern Ethiopia were correlated with the peak regional metamorphism at pumpellyite–actinolite to lower greens schist facies (Alene, 1998; Alene and Sacchi, 2000; Alene et al., 2006).

CHAPTER FIVE

5. DEFORMATION AND STRUCTURES

5.1 Introduction

In the study area both brittle and ductile tectonic structures are recognized (Fig.5.1-5.4). Field investigation and thin section study of structures, deformation and microstructural analysis reveals that three phase of deformations (D1, D2, and D3) have been experienced in different locality of the mapped area. These polyphase deformation structural patterns are marked by the existence of NE striking foliation, folds and lineation. First phase deformation (D1) is represented by the existence of foliation (S1) and by composite fabric development in which the schistosity and the original layering (S_0) are parallel. Second phase deformation (D2) is represented by crenulation lineation, plunging folds and kink folds. Third phase deformation is defined by brittle structural elements.

5.2 Primary structures

5.2.1 Bedding, lamination and Tuffaceous layers

Bedding, laminations and tuffaceous layers are preserved primary structures in some lithological units (Fig.5.1) and these structures have various color, composition and thickness. Tuffaceous layer (Fig.5.1A) displays layer of light grey tuff and weakly foliated weathered felsic agglomerates with variable (30 to 70cm) thickness.

Bedding in slate rock unit (Fig.5.1B) shows variable thickness of beds with N-E striking and dipping 40º to west. Thin laminations are visible in metalimestone out crop photo (Fig.5.1C) with black and gery color variations. Thin section study (Fig.5.1 D) also support the existence of lamination in this rock unit.

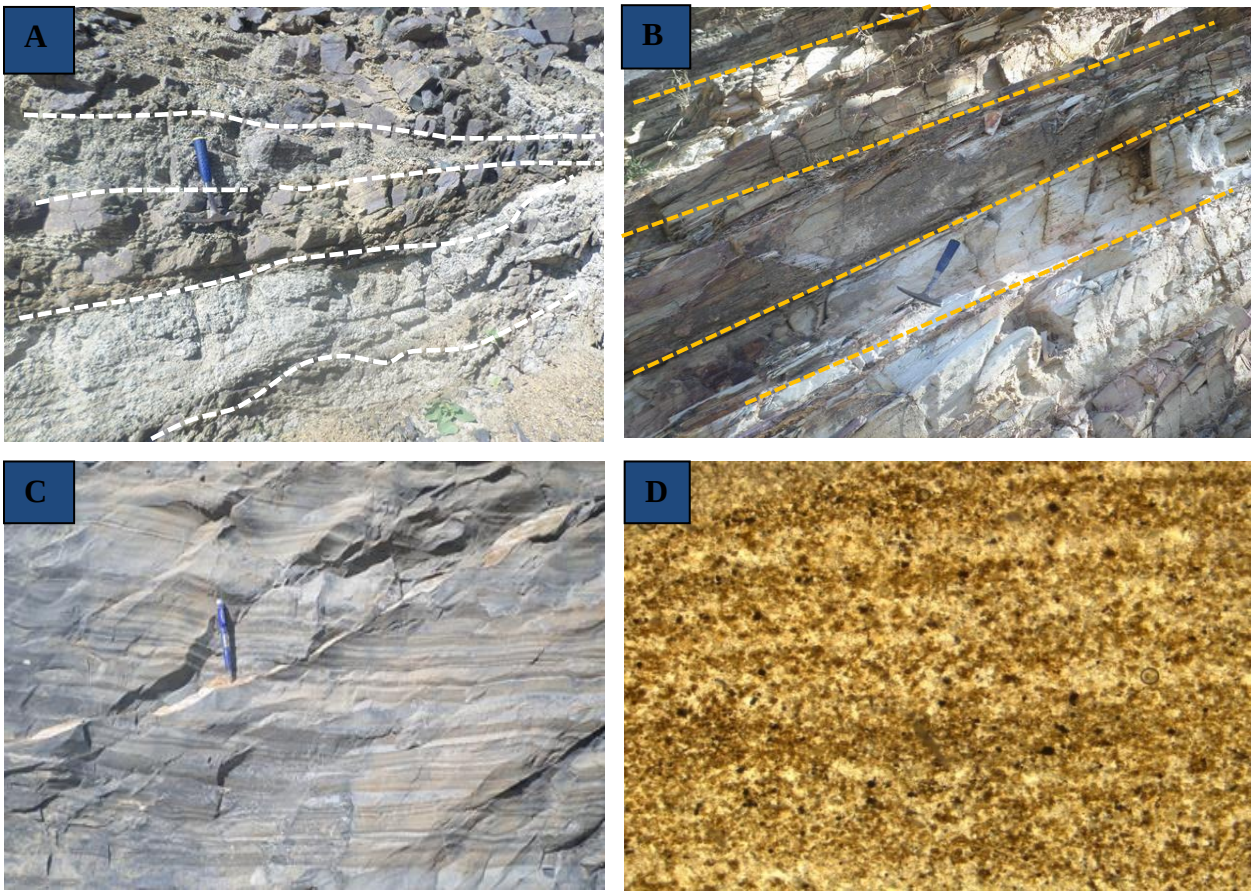

Figure 5.1 Field photographs of primary bedding lamination and tuffaceous layers in various units from different locations A) tuffaceous layer with variation in colors, photo taken facing to west at location (0498494E, 1527374N), B) variable thickness of beds in slate unit photo taken facing to north at location (0503740E, 1520250N), C) metalimestone unit displaying laminations photo taken facing west at location (0495206E, 1527989N), D) displays thin lamination in meta-limestone rock unit from sample # W11 under PPL view with (40x magnification).

5.2.2 S0 /S1 Fabric

Compositional layering (S0) is common in metalimestone and graphitic slate rock units (Fig.5.2 A and B).These primary layers are revealed by alternating concentrations of mica-rich/clay-rich and calcite layers for metalimestone (Fig.5.2A). A mica-quartz rich domain in graphitic slate (Fig.5.2B) shows S1fabric development with considerable variation in thickness and composition of individual beds.

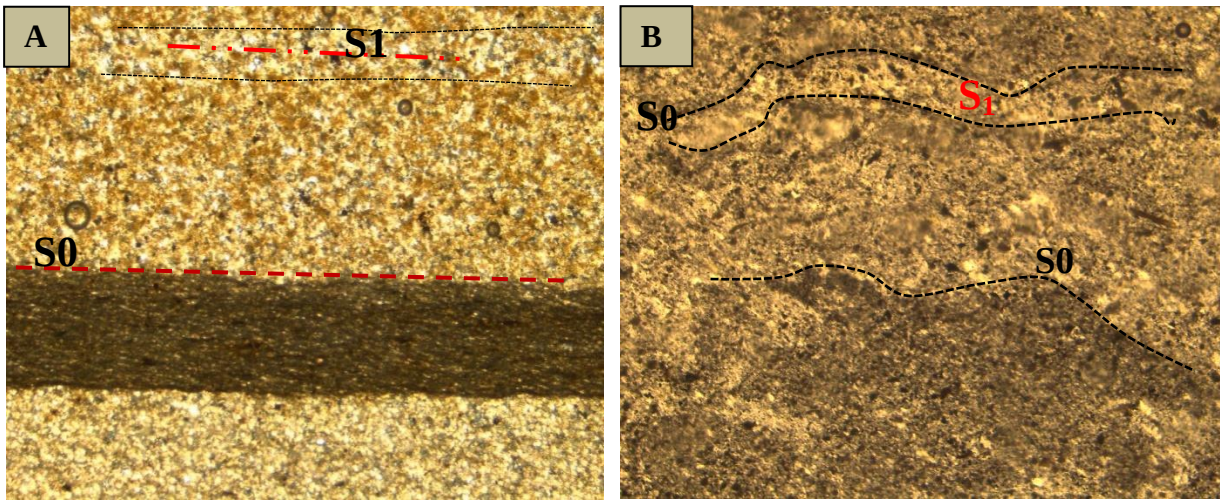

Figure 5.2 Microphotographs showing foliation defined by compositional banding under XPL view with (40x magnifications) A)Displays primary laminated bed of metalamestone (0495206E,1527989N) with alternating layer between clay rich bed and fine grain calcite rich fabrics. Calcite rich fabrics(S1 foliation) is parallel to primary clay rich bed B)shows slaty cleavage described by alternate bands of quartz and mica-rich domains graphitic slate(0497053E,1527803N) S1 foliation is slightly developed parallel to primary bed with variable thickness.

5.3 First phase deformation (D1) and associated structures

5.3.1 S1Foliation

S1 foliation is the major structural feature in the study area and general trend of northeast striking and variably northwest to southeast dipping. It is typical structure almost throughout the majority of lithologic units but, more developed in graphitic slate, foliated tuff and metaandesitic rock units (fig.5.2A-D).

Continuous cleavage in graphitic slate (fig.5.2 A and B) exhibits S1foliation.

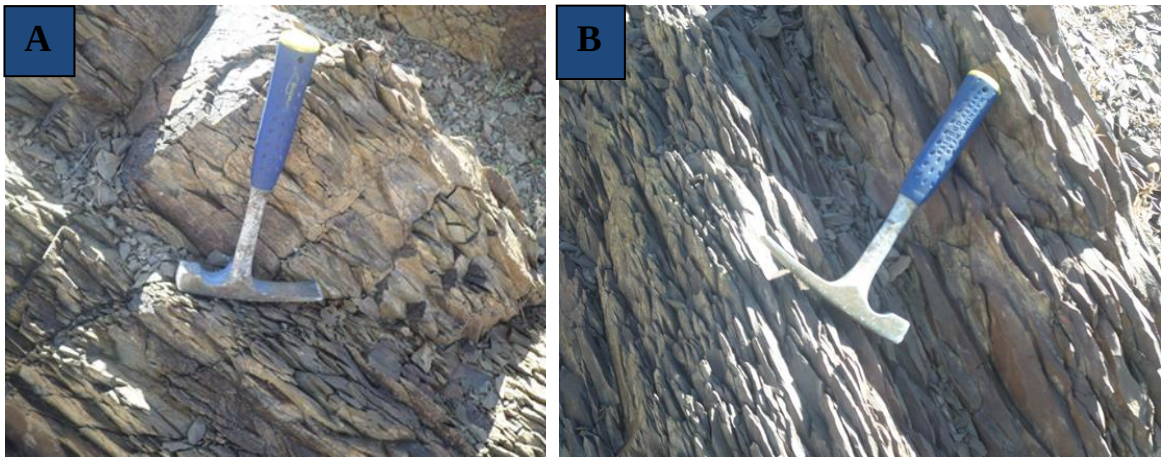

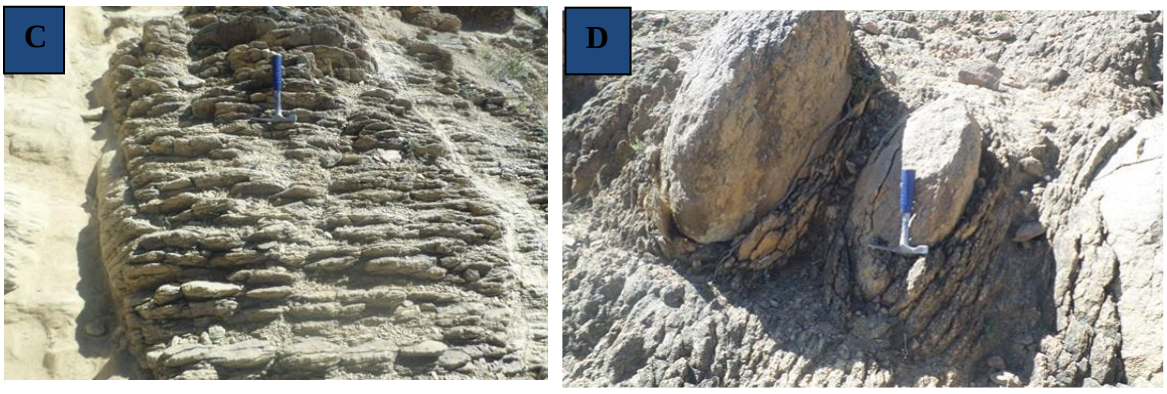

Figure 5.3 Field photographs of S1 foliation in different lithologic units A) well developed continous cleavage in graphitic slate photo taken facing east at location of (0496682E, 1527569N)B) out crop photo of slaty cleavage in graphitic slate photo taken facing east at location of (0497053E, 1527806N) C)out crop photo of foliated tuff in intercalated layer of tuff and metabasaltic rock unit that reveals S1 foliation at location of (0498973E, 1527390N) and D) well developed S1 foliation in intercalation of tuff with metaandesite rock unit photo taken facing south at location (050045E,1524081N).

5.4 D2 structures

5.4.1 S2 foliation

S2 foliation is ductile type structures which are common in phyllite rock unit of the study area. These structural features are described from field observation and microscopic study of thin sections. Micro structural analysis under thin section (Fig.5.3 A) reveals that S2 foliation is designated by continuous realignments of fine-grained platy minerals and it has cross cutting relationship with the regional (S1 foliation).Here we can realize that earlier deformation (D1) has produce foliation and later deformation (D2) has crenulated to successive micro folds with parallel fold axis. Therefore understanding the relationship between S2 foliation and phase of deformation with mineral assemblages enables to evaluate metamorphic and tectonic evolution of the area.

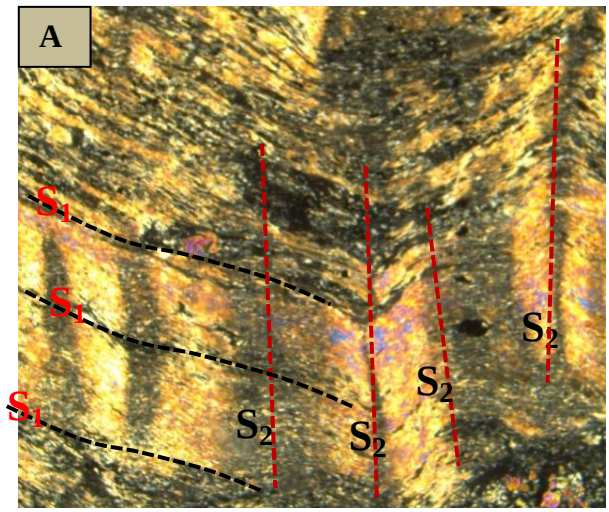

Figure 5.4 A Microphotographs of phyllite showing crenulation (sample W20, 40x, XPL 0503971E, 1521677N).

5.4.2 F2 folds

The F2 folds are well exposed in various lithologic units in the study area and these types of fold are characteristically, sub horizontal to moderately plunging folds and kink folds (Fig.5.3A-F). In metalimstone rock unit (Fig.5.3A-D) folds occur in a centimeter to meter scale synforms and antiforms throughout the out crop. Moderately plunging folded quartz vein is observed within the intercalated layer of foliated tuff and metabasalt rock units (Fig.5.3E). Typical kink fold also found in phyllite rock unit of the study area (Fig.5.3F) which characterized by straight limbs with sharp angular hinges.

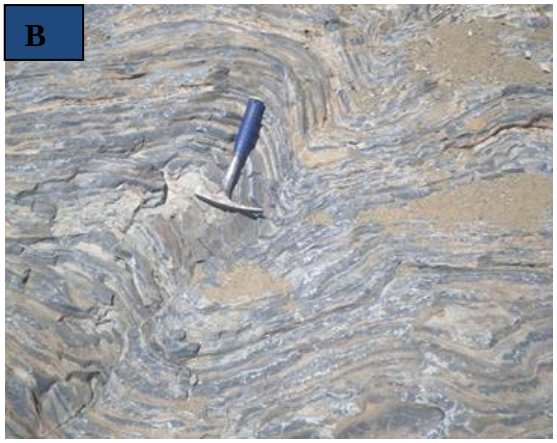

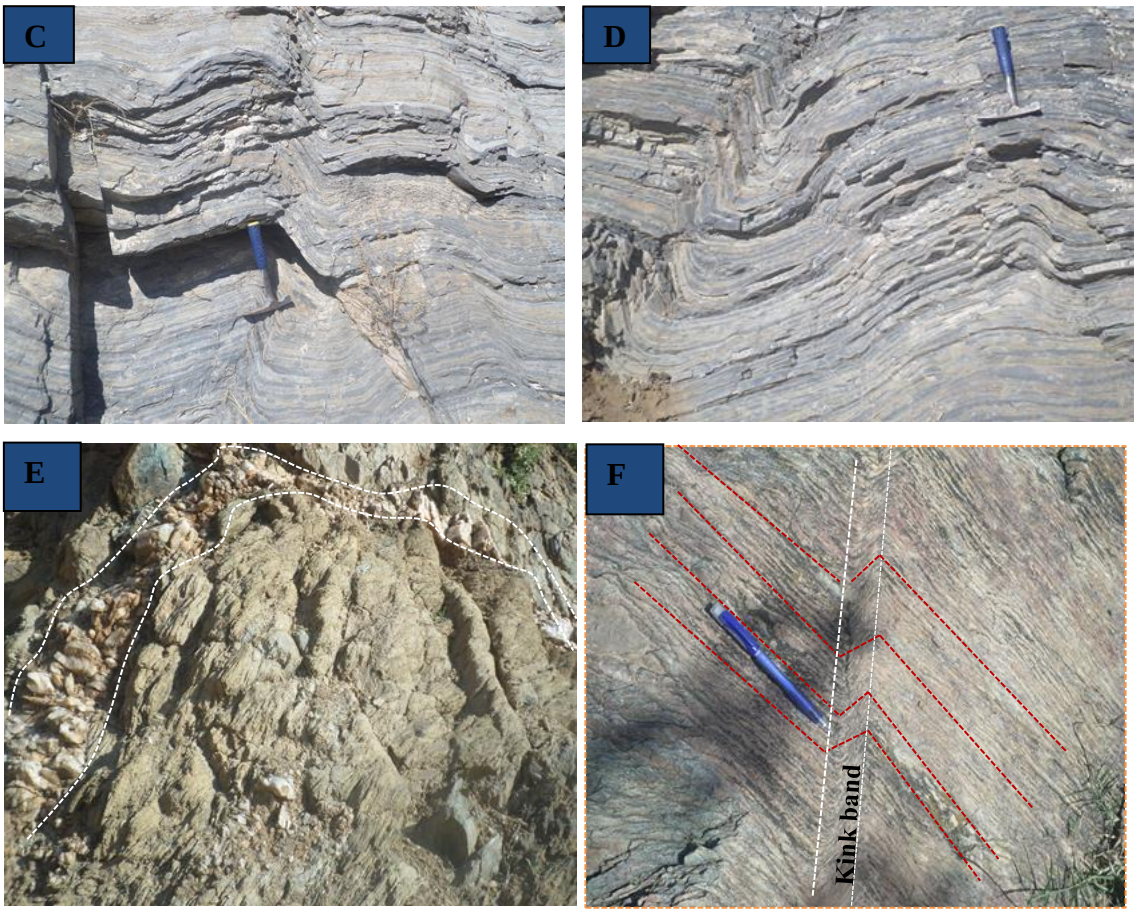

Figure 5.5 field photos of mesoscopic folds from different locations and lithologic units of the study area. A) plunging fold within metalimestone rock unit plunging 05^0 towards 165^0 with A.P 185/75SE at location of (0499506E, 1527969N) photo taken facing south west, B) sub horizontal fold (08^0 towards 195^0) with A.P 190/70 SE in metalimestone rock unit at location (0499506E, 1527980N), photo taken facing south west C) plunging fold within metalimestone rock unit plunging 08^0 towards 184^0 with A.P 190/60SE at location of (04999508E, 1528008N) photo taken facing SW, D) a fold with moderately plunging fold axis (15^0 towards 200^0) with A.P 180/54SE within metalimestone rock unit at location of (0499506E,1527980N) photo taken facing SW, E) Fold quartz vein with open moderate plunging fold axis(35^0 towards 060^0) in intercalated layer of foliated tuff and metabasalt rock unit at location of (0503208E, 1520422N) photo taken facing north and F) kink fold within phyllite rock unit at location of (0504196E,1522253N) photo taken facing east.

5.5 Post –D2 structures

5.5.1 Veins and joints

Two set of joints and fractures are common brittle structural features through all lithological units in the study area. From field observations and thin section study some joints are filled by secondary minerals (Fig.5.4 A and D). These structures shows that they have cross cut relationship with regional foliation (see Fig. 5.4 A and D).

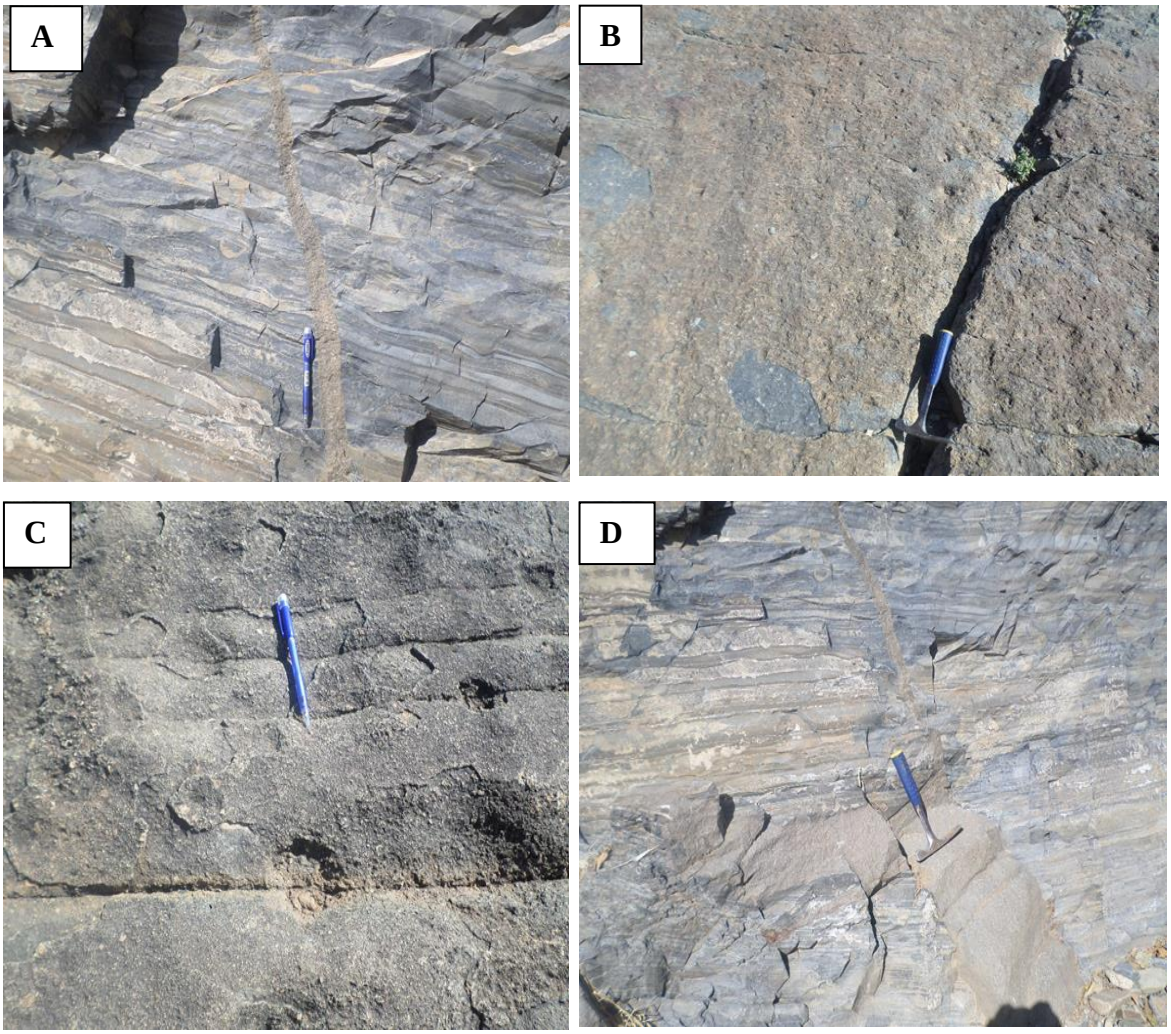

Figure 5.6 field photos of different joints in the study area with different orientations.

A) photo in metalimestone rock unit shows two set joints that the vertical one is filled by mica mineral but the top horizontal joint is not filled at location of (0495206E,1527989N) photo taken facing to southwest, B) out crop photo of two set joint within metabasic rock unit at location of (0496679E,1522175N) photo taken facing toeast, C) reveals one set parallel joints with the same orientation in metabasic rock unit (0498377E,1520201N) photo taken facing to north, D)joint filled with

mica mineral which shows wide aperture at the base and narrow to the top part of the metalimestone bed, photo taken facing to southwest.

5.5.2 Micro veins

The study area is characterized by large number of quartz veins with different orientation throughout different lithological units. Microscopic study of these rocks shows a variety of deformed quartz veins (Fig.5.7 A-D) and these veins have variable relationships with foliations of the rock. Understanding the relationship between deformed veins and foliation can be used to realize about the metamorphic evolution and deformation process.

The first plates folded quartz vein (Fig.5.7 A and B) under PPL and XPL view shows that the vein is not altered whereas, in the second plates under PPL (Fig.5.7 C and D) reveals that the vein is altered to chlorite.

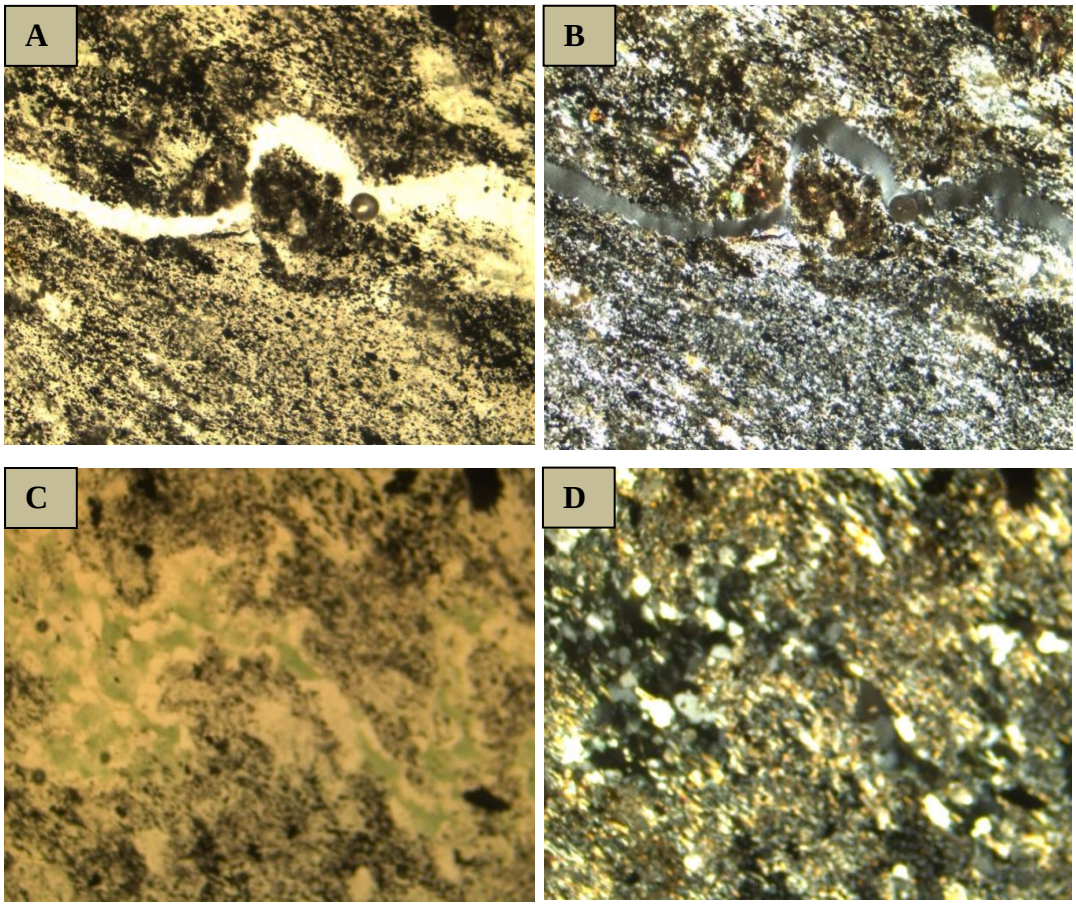

Figure 5.7 Microphotographs of folded quartz veins in phyllite(A and B) and in metabasic rock (C and D), under PPL and XPL 40x magnification.

5.7 Time relationship between deformation and metamorphism

As mentioned earlier three major planar structures (S0, S1 and S2) are well developed in the area. Minerals such as chlorite, muscovite/sericite, calcite, graphite and recrystallized quartz are associated with S1 foliation and it displays that they were formed during first phase deformation (D1).Therefore it can be said that the M1 metamorphic event is responsible for the formation of these minerals which is synchronous with the first phase deformation (D1).

The S1foliation (Fig.5.4) is folded to form S2 crenulation cleavage during D2 by slight rotation. Therefore S2 crenulation cleavage can be accommodate by synchronous with D2 deformation.

5.8 Stereographic projection and structural analysis

The general orientation of structures and correlation with regional structural framework has been understood from stereographic projection (Fig.5.6).

The equal area plots of S0 and S1 foliation as poles (Fig.5.6 A) and Contours of poles in Kamb methods (Fig.5. 6 B) shows that the majority of the poles are clustered in the South East and North West quadrants of the net. Generally these plots have been interpreted and depict that the foliation predominantly dip towards North West direction. Regionally S1 foliations are correlated with first phase of deformation (D1) which was formed as result of N-S compression (Alene et al., 2006). Another plots of the plunge of linear structures for D2 fold axis and lineation (Fig.5.6 C) both are clustered in southern part of the net and plunging shallowly with an average 12^0 towards 175^0 south. On the other hand the rose diagram plots for joint (Fig. 7) displays different orientation due to the existence of different sets of joints. These structural elements have cross cut relationship with regional foliation. Therefore joints can be associated with post-D2 deformation and considered as the youngest brittle structural features. The above mentioned structural patterns possibly indicate that the area has been experienced different phase of deformations.

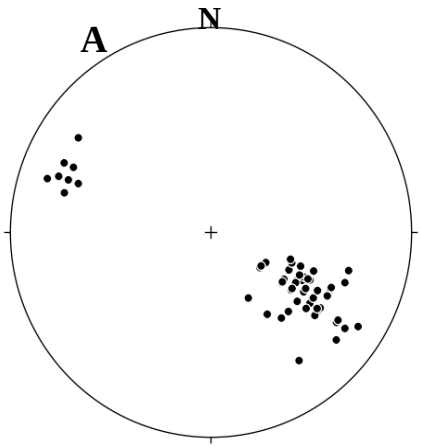

Lower hemisphere Lambert (equal area) net plots of S0 and S1 foliation as the poles. Total number of points = 60.

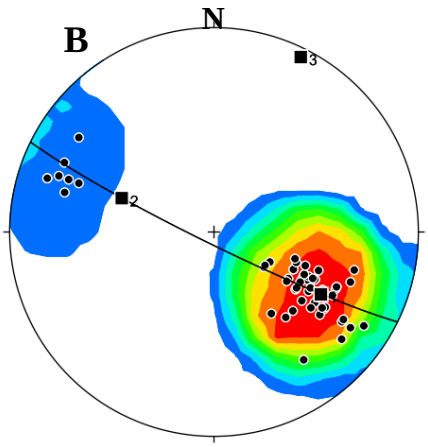

Contours of poles in Kamb methods showing gridded density of the dominant structural elements S1 foliations. Total number of points = 60.

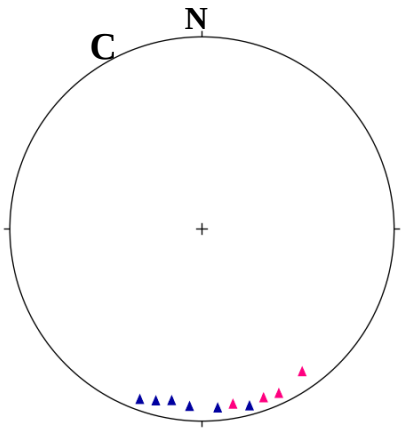

key **Bblue –D2 fold axis**

Pink –L2 lineation

Lower hemisphere Lambert (equal area) net plots of F2 fold axis and L2 lineation. Total number of points = 11.

Figure 5.8 Plots of planar structures as poles on lower hemisphere Lambert (equal area) net.

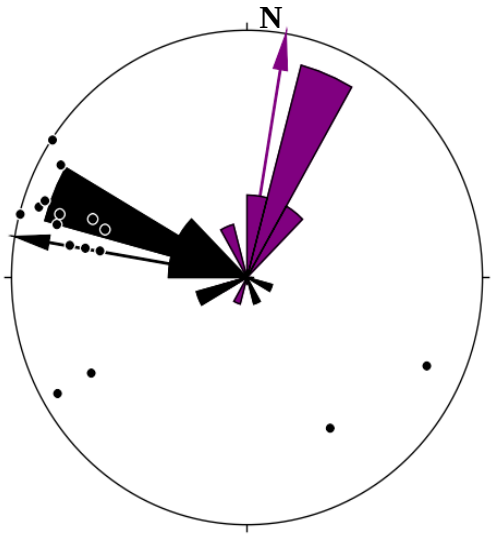

Figure 5.9 Rose diagram of different set of joints. Total number of points = 18.

CHAPTER SIX

6. GEOCHEMISTRY OF METAVOLCANICS

6.1 Analytical Methods

Twelve metavolcanic rock samples have been analyzed for their chemical compositions and source signatures. The samples were sent to Australia laboratory science (ALS) for analytical work. The whole rock elemental compositions were characterized by analytical method of inductively coupled plasma-atomic emission spectroscopy (ICP-AES) technique. The major elements and Trace elements including full rare earth element suites were quantified by using inductively coupled plasma mass spectrometry (ICP-MS) and ICP-MS lithium borate fusion is used for the resistive elements. A four acid digestion for the base metals, by (ICP-AES) and an aqua regia digestion have been used for the volatile gold related trace elements identification. Loss on ignition (LOI) at 1000^0c is determined by WST-SEQ and total carbon and total sulphur were recognized by LECO.

The sample preparation for geochemical analysis including removal of the weathered part from the surface of the rock and cutting rock to the required size were done in Addis Ababa University School of Earth Sciences thin section room. Other procedures including making a rock powder, crushing, splitting and pulverizing were conducted at the ALS.

Generally the following procedures have been used in a package in order to meet specific needs regarding sample size and composition.

Crushing: Jaw crushers were used to reduce sample particle to desirable size prior to pulverization.

Splitting: After crushing, samples were split into representative sub-samples. Automated rotary splitters attached to crushers to produce demonstrably superior precision in sub-sample analyses.

Pulverizing: All pulverizing procedures make use of “flying disk” style low-chrome steel grinding mills. The elemental composition of each rock samples, trace elements including the full rare earth element suites are determined using ICP-MS.

The major, trace and rare earth elements abundance of the twelve whole-rock samples are shown in Table 6.1. These data are used in construction of selected discrimination and variation

diagrams in order to understand their geochemical nature and predict the tectonic setting of the area.

Table 6.1 Whole rock major and trace element geochemical analysis data for metavolcanic rock samples from Workamba area.

Sample	W1	W3	W4	W5	W6	W7	W8	W9	W13	W14	W16	W19
SiO2	68.9	73.1	50.5	68.6	52.1	49.9	50	59.6	65	55.5	53.4	58.5
Al2O3	14.1	11.35	19.4	13.7	17.3	17.75	17.95	14.3	15.1	15.8	16.75	18.15
Fe2O3	5.14	4.37	8.4	4.64	10.3	11.6	11.55	8.11	5.56	8.09	9.73	5.76
CaO	1.89	2.18	9.67	3.76	6.65	5.38	5.44	6.11	5.17	9.99	8.31	2.74
MgO	0.35	0.21	3.56	0.79	3.81	2.6	2.61	1.97	1.5	3.05	3.96	2.76
Na2O	5.94	0.93	3.18	5.21	4.47	6.3	6.29	0.46	2.98	3.43	2.42	5.99
K2O	1.53	5.92	1.43	0.34	0.12	2.02	1.96	3.21	2.03	0.06	1.71	2.71
Cr2O3	<0.01	<0.01	0.01	<0.01	<0.01	<0.01	<0.01	<0.01	<0.01	<0.01	<0.01	<0.01
TiO2	0.67	0.44	0.91	0.51	1.08	2.66	2.69	0.78	0.62	1.03	1.18	0.57
MnO	0.03	0.07	0.11	0.06	0.17	0.16	0.16	0.12	0.11	0.16	0.15	0.06
P2O5	0.21	0.11	0.41	0.18	0.5	0.87	0.85	0.26	0.2	0.4	0.45	0.43
SrO	0.02	0.12	0.1	0.16	0.01	0.14	0.14	0.17	0.46	0.16	0.09	0.05
BaO	0.15	0.16	0.07	0.02	0.01	0.05	0.05	0.24	0.11	0.01	0.11	0.14
LOI	0.79	0.66	3.13	1.68	4.68	1.34	1.14	3.47	1.94	3.53	3.09	1.97
Total	99.72	99.62	100.88	99.65	101.2	100.77	100.83	98.8	100.78	101.21	101.35	99.83
Li	<10	<10	10	<10	30	10	10	10	<10	10	10	<10
C	0.03	0.05	0.02	0.24	1.11	0.03	0.02	0.96	0.04	0.39	0.06	0.03
Sc	13	10	18	12	29	9	8	21	14	26	25	10
V	25	15	221	54	179	64	67	105	83	244	271	103
Cr	30	20	100	30	10	20	10	30	20	20	30	30
Co	5	3	25	9	25	25	26	22	9	25	28	15
Ni	<1	7	29	3	3	5	6	11		10	16	12
Cu	22	22	148	36	87	50	49	91	123	312	91	69
Zn	65	77	79	55	116	115	116	87	67	83	106	80
Ga	14.8	16.1	21.2	12.8	19.5	22.5	22.6	15.6	17.8	19.9	22.1	20
Ge	<5	<5	<5	<5	<5	<5	<5	<5	<5	<5	<5	<5
As	0.7	3.2	7.8	2.4	5.1	0.8	0.8	7.1	4.8	2.7	0.3	0.3
Se	0.4	0.2	0.3	0.2	<0.2	0.8	0.8	<0.2	<0.2	0.4	0.5	0.6
Rb	21.7	73.1	33	7.8	1.5	33.7	33.5	33.6	51.9	1.2	28.6	31.3
Sr	233	977	889	1310	139	1180	1215	1375	3900	1350	823	490
Y	22.1	23.8	19	17.3	20.5	47.1	45.5	15.2	19.9	17.1	21.3	16.1
Zr	145	138	73	100	77	458	437	56	113	82	103	129
Nb	6.5	3.7	1.7	2.2	1.3	36.8	35.3	0.6	2.9	3.8	6.5	2.8
Mo	1	1	1	<1	1	2	2	1	<1	<1	1	<1
Ag	<0.5	<0.5	<0.5	<0.5	<0.5	<0.5	<0.5	<0.5	<0.5	<0.5	<0.5	<0.5
Cd	<0.5	<0.5	<0.5	<0.5	<0.5	<0.5	<0.5	<0.5	<0.5	<0.5	<0.5	<0.5
In	0.016	0.016	0.011	0.008	0.026	0.029	0.028	0.019	0.014	0.016	0.017	0.007
Sn	1	1	1	1	1	4	3	2	1	1	2	1
Sb	0.07	0.25	0.4	0.08	0.07	0.07	0.07	0.2	0.2	0.74	0.05	0.08
Te	<0.01	0.01	0.01	0.02	0.02	0.01	0.02	0.04	0.05	<0.0	<0.0	<0.01
Ce	56.7	36.9	29.4	27.7	30.8	105	104	18.2	32.9	40.9	43.9	54.4
Pr	6.87	4.49	3.87	3.36	4.04	13.85	13.55	2.57	4.04	5.17	5.68	6.38
Cs	0.92	0.75	1.33	0.21	0.1	0.7	0.81	0.73	1.12	0.14	0.86	0.63
Ba	1365	1445	567	177.5	78.4	403	400	2180	961	70.6	975	1395

La	31.9	18.2	14	14.3	15	46.3	45.2	9	17.6	20.1	21.7	30.5
Ce	56.7	36.9	29.4	27.7	30.8	105	104	18.2	32.9	40.9	43.9	54.4
Pr	6.87	4.49	3.87	3.36	4.04	13.85	13.55	2.57	4.04	5.17	5.68	6.38
Nd	28.4	20	17.8	13.9	19.5	61.6	58.6	12.3	17.2	22.6	25.7	26.4
Sm	5.32	4.21	3.84	3.22	4.4	13.35	13.55	2.8	3.92	4.67	5.64	4.73
Eu	1.14	1.07	1.38	0.97	1.43	4.2	4.35	1.02	1.09	1.39	1.57	1.28
Gd	4.81	4.44	4.15	3.1	4.43	12.45	12.35	2.97	3.57	4.03	4.7	3.85
Tb	0.69	0.74	0.61	0.54	0.66	1.88	1.78	0.48	0.55	0.61	0.68	0.54
Dy	4.12	4.31	3.56	3.32	4.07	10.4	10.2	3.06	3.55	3.48	4.24	3.02
Ho	0.79	0.93	0.71	0.65	0.79	1.88	1.85	0.58	0.71	0.62	0.78	0.55
Er	2.22	2.6	1.88	1.75	2.27	4.71	4.56	1.6	2.05	1.91	1.91	1.56
Tm	0.34	0.43	0.29	0.3	0.32	0.58	0.59	0.22	0.31	0.26	0.3	0.22
Yb	2.33	2.6	1.82	1.99	2.22	3.8	3.42	1.73	2.08	1.64	2.05	1.6
Lu	0.38	0.43	0.24	0.3	0.33	0.52	0.53	0.2	0.34	0.22	0.3	0.21
Hf	4.5	4.1	2.2	2.9	2.3	11.6	10.5	1.6	3.4	2.2	3	3
Ta	0.4	0.3	0.1	0.2	0.1	2.1	2.1	<0.1	0.2	0.2	0.4	0.2
W	2	3	2	<1	<1	<1	1	<1	2	1	1	2
Re	0.001	<0.001	<0.001	<0.00	<0.001	<0.00	<0.00	0.001	<0.00	<0.001	<0.001	<0.001
Hg	<0.005	0.017	<0.005	<0.005	0.022	<0.005	<0.005	0.031	<0.00	0.005	<0.005	<0.005
Tl	0.02	0.02	<0.02	<0.02	<0.02	0.05	0.04	<0.02	0.02	<0.02	<0.02	0.03
Pb	9	11	2	12	10	<2	4	12	9	13	8	6
Bi	0.01	<0.0	<0.01	0.01	0.01	0.01	0.01	0.04	0.05	0.01	0.01	<0.01
Th	4.39	2.93	1.41	2.78	1.97	4.41	4.17	1.11	2.93	2.39	2.51	3.2

The major element (including LOI) and trace element value of concentration is expressed by wt. % and ppm respectively.

6.2 Rock geochemical characteristics

6.2.1 Major Oxide Characteristics

Although the metavolcanic rocks in study area subjected to green schist facies metamorphism and extensive deformations, Harker-type variation diagrams in (Fig. 6.1a-h) which is plotted for major oxides against Silica (SiO_2wt %) that major oxides, (MgO, TiO2, Fe_2O_3t, CaO, Al_2O_3), P_2O_5 and MnO are negatively correlated with increasing SiO_2, (normal differentiation trend).This suggests that olivine, pyroxene, magnetite, and calcic plagioclase were major fractionating phases during evolution of the magma. Conversely, K_2O and Na_2O show a scattered pattern with the progressive increasing in silica contents which are incompatible with the presence mafic minerals. These metavolcanic rocks of the study area also characterized by wide compositional range of major oxide concentrations (Table 6.1), for example SiO_2 contents fall within wide range (49.9–73.1 wt. %) from basalt to rhyolite fields and these sequence basalt to rhyolite are common for the subalkaline series (Winter, 2001).

The metavolcanic rocks are also characterized by high iron (Fe_2O_3) contents (4.37-11.6 wt %) and this high iron-oxide contents may related to varying degree of later alteration (e.g. oxidation). TiO_2 (0.44-2.69 wt %) in (Fig.6.1b) after initial enrichment of TiO_2 concentrations and abrupt decreasing indicate the crystallization of Ti-bearing pyroxene and Fe-Ti oxides. These results also show high-alumina (Al_2O_3) contents from 11.35 wt % up to 19.4 wt %, (17-21 %) values similar to those of calc-alkaline series rocks (Irvine and Baragar, 1971).

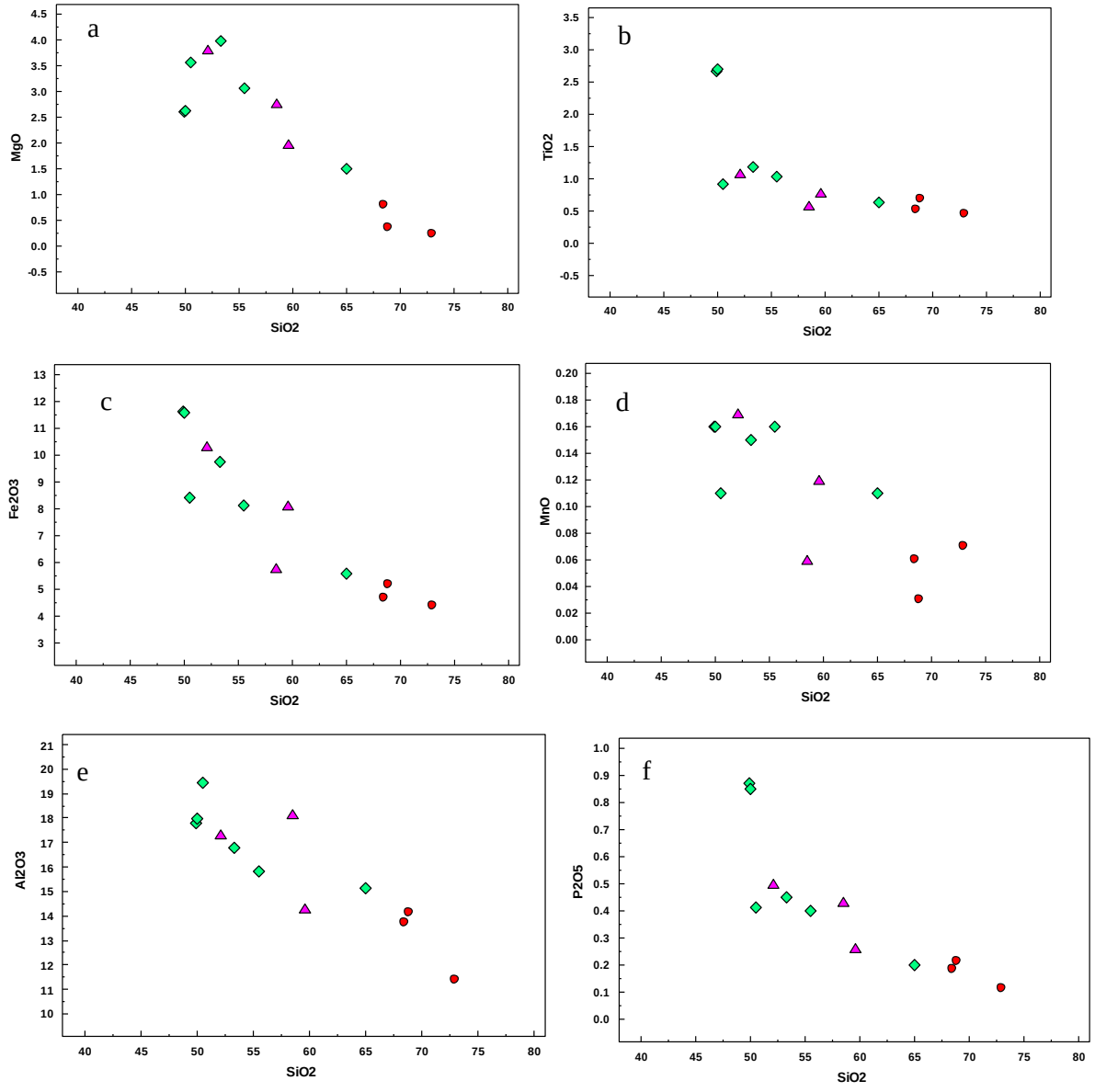

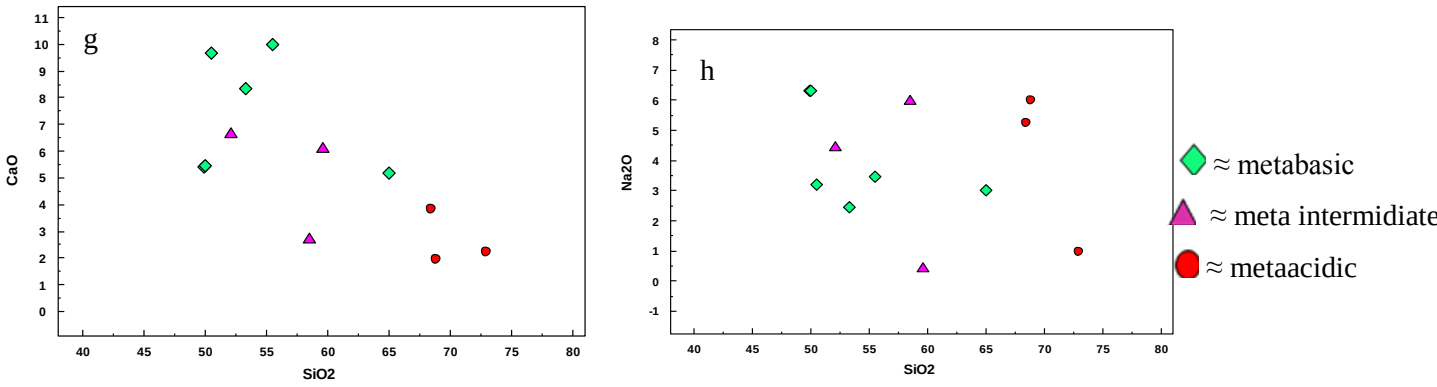

Figure 6.1(a-h) Harker-type variation diagrams for major element oxides-SiO_2 (wt %).

6.2.2 Trace and Rare Earth Element Characteristics

The Harker variation diagrams plotted for selected trace elements (Nb, Ni, Sc, Zr, Y, Ba, and Sr); Ba and Rb reveal fairly linear positive correlation with SiO_2, whereas compatible trace elements(Ni, Sc) shows invers correlation because of partitioning of olivine, spinel and pyroxene. The (HFS) elements Nb, Zr, and Y, also displays slightly positive correlation with SiO_2, which indicates that during metamorphism and other alteration processes they were immobile and remain almost unchanged. Trace and rare earth element concentrations of metavolcanics from the study area also show considerable wide variation and ranges (e.g.Ti (0.44-2.69 ppm), Nb (0.6 -36.8 ppm), Y (15.2-47 ppm), Hf (1.6-11.6)).The high field strength elements (HFSE) such Ti, Nb, Hf and Y, abundance is generally low and their limited concentration may reflects secondary alteration. Conversely LILE, Ba, Rb and Sr contents, shows scatter pattern with increase in silica content and it can be due to some degree of mobility (Cann, 1970). All metavolcanic rock samples of the study area shows the ratio of Y/Nb >1(Table 6.1) typical of calc-alkaline and tholeiitic basalt (Gracia, 1978) and in the Zr versus Ti tectonomagmatic discrimination diagram of Pearce and Cann (1973), almost all the sample plots in the calc-alkaline lavas field except one (Fig.6.2A).

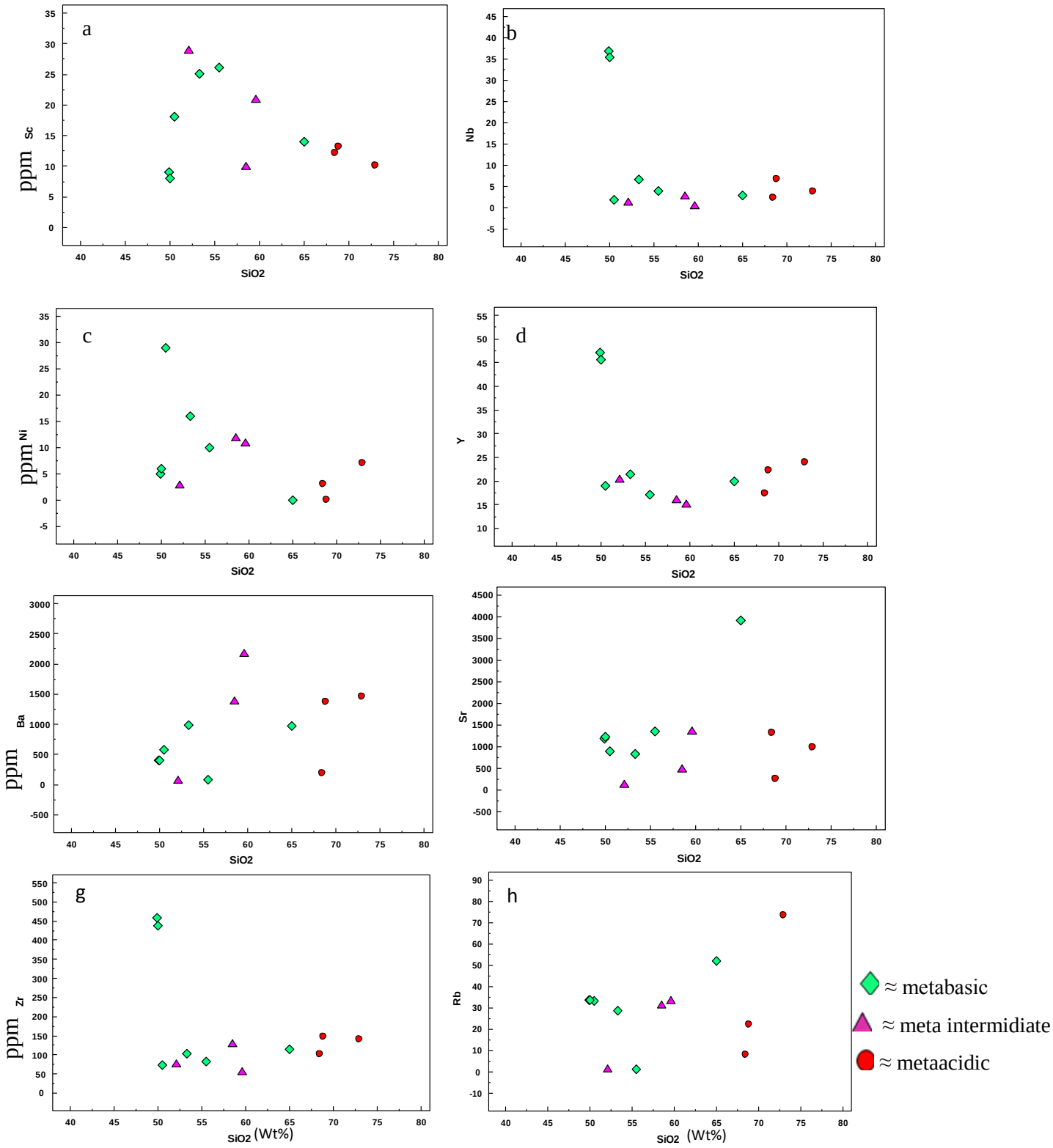

Figure 6.2 (a-h) Harker-type variation diagrams of selected trace elements (ppm) -SiO_2 (wt%) for the metavolcanics of the study area.

The REE patterns and their stability during alteration and metamorphism make them valuable indicators of magmatic affinity for metavolcanic rocks (Rollinson, 1993). High field strength elements (HFSE) Ta-Nb–Ti, in multi-element diagrams (Fig.6.3A) shows negative anomaly. Light REE enrichment and HFSE (Ta-Nb–Ti), depletion are typical of calc-alkaline affinity and commonly interpreted to have derived from arc (Gale and Pearce, 1982). In Primitive mantle - normalized multi-element (spider) diagram (Fig.6.3A) progressive depletion in Ti from basic to acidic probably reflects preferential crystallization of Fe–Ti oxide.

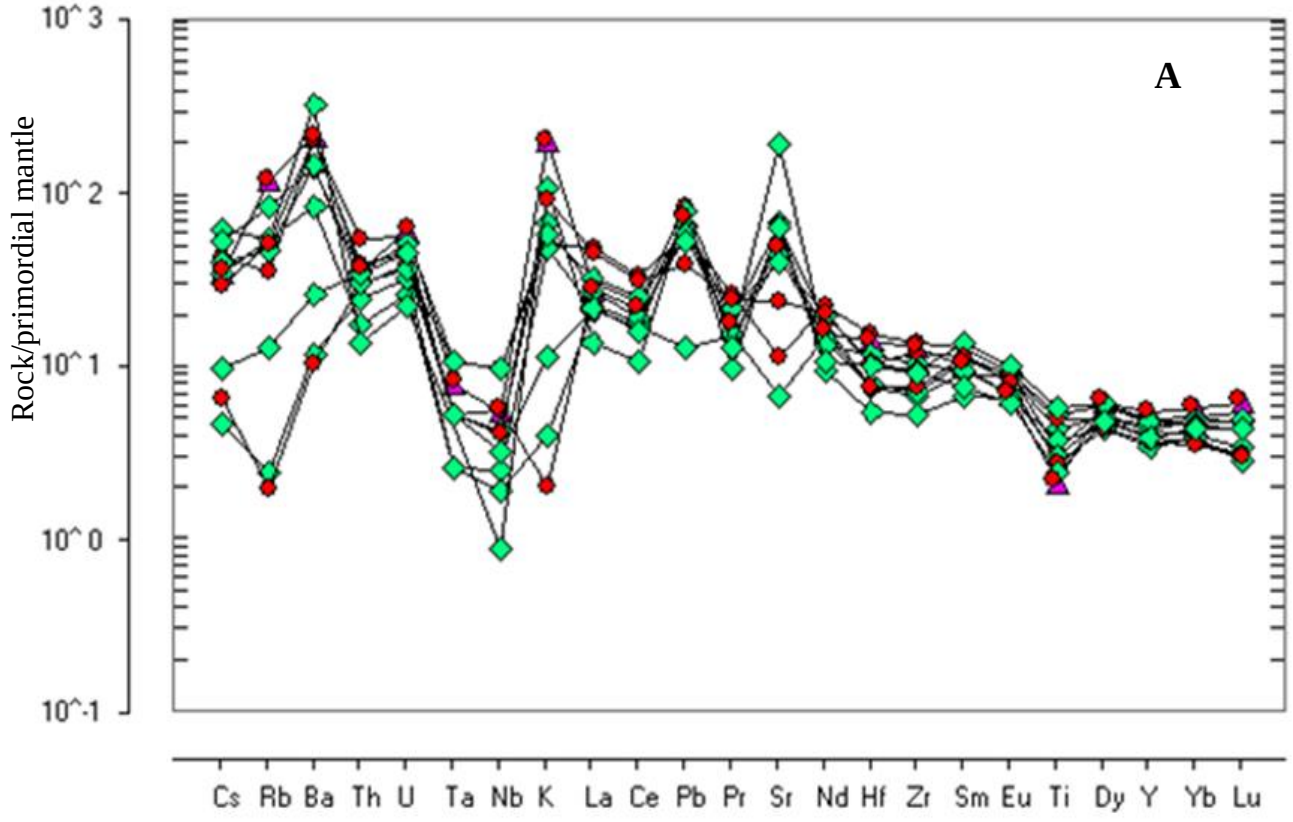

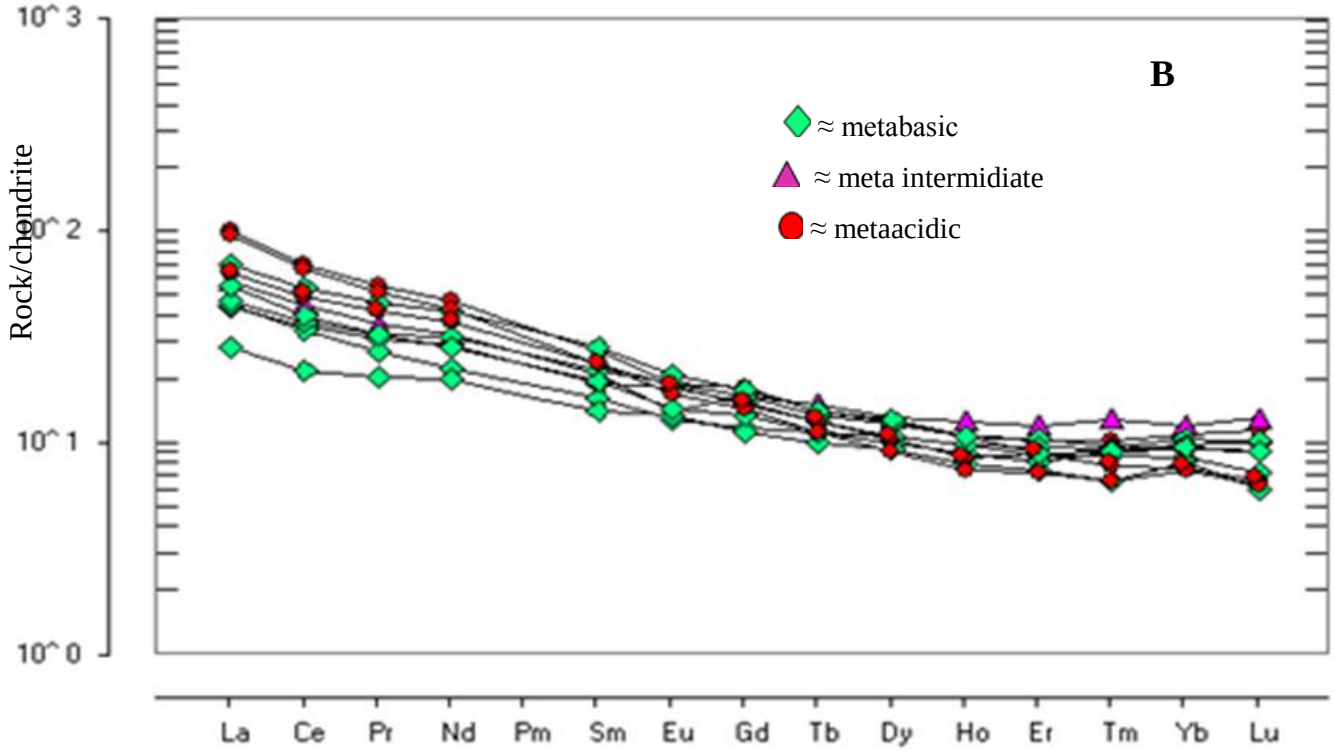

Figure 6.3 A) Primitive mantle -normalized multi-element (spider) diagram of the representative metavolcanic rock samples from the study area. Primordial mantle –normalized values are from (McDonough and Sun, 1995) and B) Chondrite- normalized REE diagram for the metavolcanic rocks, Chondrite normalization values are from Sun and McDonough (1989).

6.3 Paleotectonic Setting of the Metavolcanics

Tectonic discrimination diagrams of geochemical data for the metavolcanic rocks of Workamba area displays the chemical characteristics of the magmas generated at subduction-related settings. The Y versus Cr binary and Th-Hf-Nb tertiary geochemical discrimination diagrams of metavolcanic rocks the area (Fig.6.4B and C) indicate these rocks are subduction-related arc types (Wood, 1980). Another binary Zr versus Ti tectonomagmatic discrimination diagram (Fig.6.4A) after Pearce and Cann, (1973) shows metavolcanic rocks of the study area fall within calc-alkaline lavas field. Their calc-alkaline nature also shown by strong enrichment of low ionic potential elements Ba, Th, K and U (Fig.6.3A) and depletion in elements of high ionic potential elements Nb, Ta, Ti, REE (Fig.6.3A). The suite shows LREE enrichment increasing from mafic to felsic compositions.

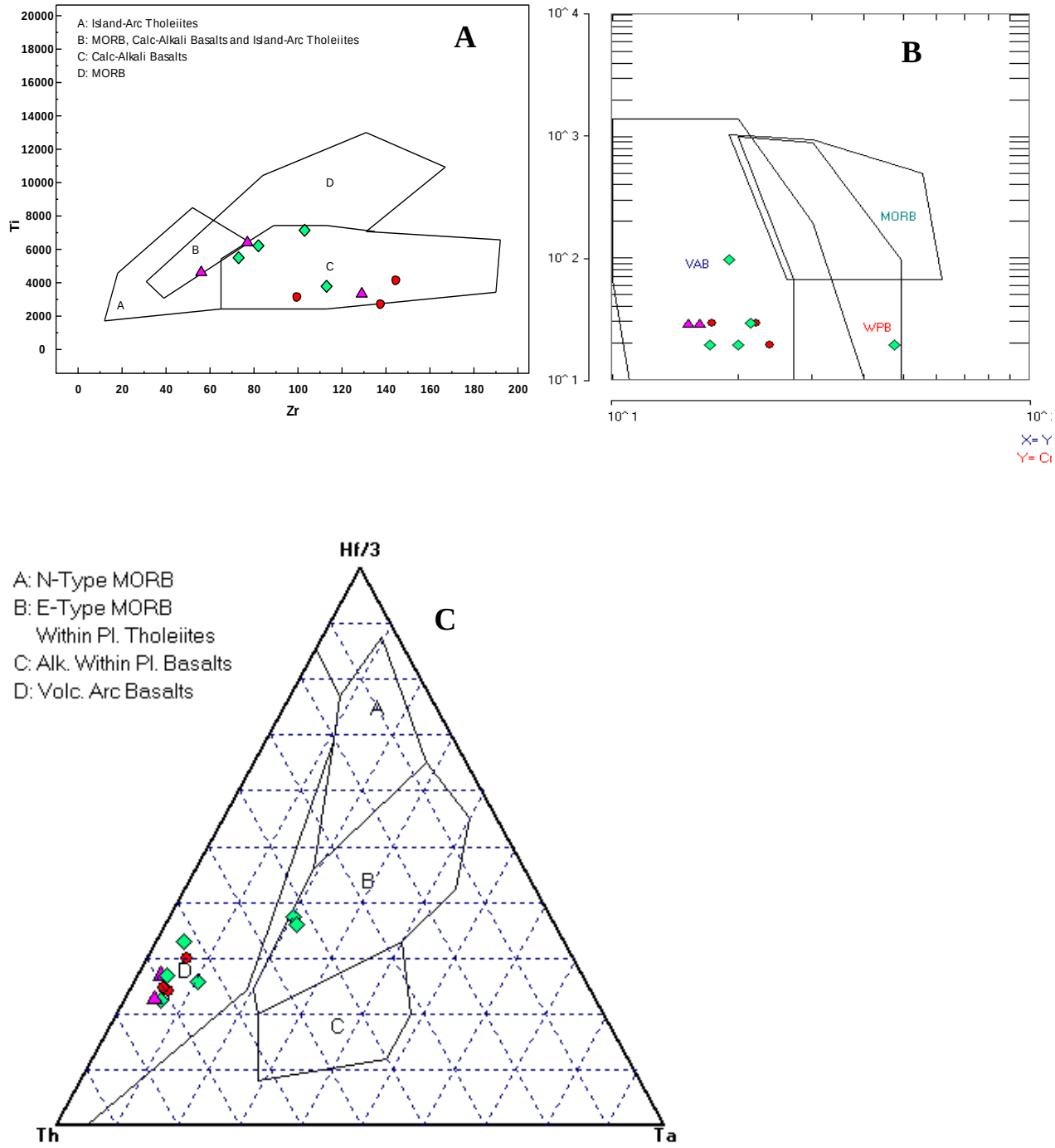

Figure 6.4 Tectonic discrimination diagrams for the metavolcanic rocks of the study area.

Diagrams after A) Pearce and Cann, (1973), B) Pearce, (1982), C) after Wood (1980) where, Abbreviations for all plots: MORB = mid-ocean ridge basalt, VAB = volcanic-arc basalt, WPB = within plate basalt.

In general several researchers (e.g. Alene et al., 1998;Alene et al., 2000; Asrat et al, 2001; Avigad et al., 2007; Miller et al., 2012; Sifeta et al., 2005;Tadesse et al., 1999; Tadesse et al., 2000) shows the Tsaliet Group of northern Ethiopia represents an arc volcanics sequence or subduction-related arc accretion of the ANS.

The geochemical data for metavolcanic rocks of Workamba area in northern Ethiopia shows the calc-alkaline affinity with arc-related geochemical signatures.

In this study geochemical results are supportive evidence with petrographic and structural analysis to predict deformation history of Workamba area and to correlate with the regional works.

CHAPTER- SEVEN

7. CONCLUSION AND RECOMMENDATIONS

7.1 Conclusion

From field observation and mapping, petrographic, structural and geochemical analysis the following conclusion has been made about Workamba area. The study area consists of foliated and non-foliated metabasalt, metabasaltic-andesite, metavolcaoclast, metabrecia, graphitic slate, micaceous slate, phyllite and metalimestone rock units but, most part of the area is covered by metavolcanic rocks. Based on index mineral assemblages; chlorite, actinolite, epidote, muscovite and serisite which established from petrographic analysisit interpreted as the rocks in the study experienced low grade metamorphism (green schist facies metamorphism). Preservation of igneous relicts and textures, primary structures like bedding and compositional layering are another evidence for low grade alterations. These metavolcano-sedimentary rocks also have been subjected to poly phase deformation.

In this study petrographic investigation from selected rock samples, structural and kinematic analyses enables to conclude that deformation history of the area was proceed with two phases of ductile deformation (D1 and D2) and later affected by third phase (D3) brittle deformation. The time relationship between metamorphism and deformation is interpreted from mineral assemblages and micro-structural features. The first phase deformation (D1) is established by NE striking S1foliation and associated with M1metamorphism minerals developments such as chlorite, epidote, actinolite, muscovite/sericite, calcite, graphite and recrystallized quartz. Therefore from these associations we can conclude that regional M1 metamorphic event is responsible for the formation of these minerals which is synchronous with the first phase deformation (D1).

The second phase deformation D2 is characterized by the local development of low plunging folds, S2 cleavage and kink fold. During D2 deformation S1foliation is folded to S2 crenulation cleavage by slightly rotation and recrystallization of platy minerals i.e., micas hence S2 crenulation cleavage can be accommodate by M2 metamorphic event synchronous to D2 deformation. The third phase deformation (D3) is related to different set of joints that cross cut the regional foliation throughout each rock units.

The geochemical data plotted on different tectonic discrimination diagrams clearly reveals that metavolcanic rocks of Workamba area are characterized by typical calc-alkaline suites.

The general petrological and geochemical characteristics of the Workamba metavolcanic rocks provided in an important evidence to consider the area as part of the arc volcanics sequence or subduction-related arc accretion of the ANS.

7.2. Recommendations

- Stratigraphic sequence among different section of the Tsaliet Group is not yet differentiated therefore large scale mapping and isotope data of the area is required to know stratigraphic sequence and boundary relationships through different lithologic units.
- For the Tsaliet Group of the study area there is no any local radiometric data existed hence radiometric data for age determination and to reconstruct the stratigraphic order of the area also recommended.
- The study area is enriched in veins and rocks show mineralization that is recommended to explore economic minerals.

References

Abdelsalam, M.G. and Stern, R.J. (1996). Sutures and shear zones in the Arabian- Nubian Shield, Journal of African Earth Sciences. 23: 289-300.

Alemu, T., 1998. Geochemistry of Neoproterozoic granitoids from Axum Area, northern Ethiopia. Journal of African Earth Sciences 27, 437-460.

Alene, M. 1998. Tectonomagmatic evolution of Neoproterozoic rocks of the Maikenetal- Negash area, Tigray, Northern Ethiopia. PhD thesis,University of Turin, Italy.

Alene M., Ruffini R.and Sacchi R. (2000a).Geochemistry and geotectonic setting of Neoproterozoic rocks from northern Ethiopia (Arabian-Nubian Shield), Gondwana Research. **3**: 333-347.

Alene, M., Ruffini, R., Sacchi, R., (2000).Geochemistry and geotectonic setting of Neoproterozoic rocks from northern Ethiopia (Arabian–Nubian Shield). Gondwana Res. 3, 333–347.

Alene, M., Jenkin, G.R.T., Leng, M.J., Darbyshire, D.P.F., (2006). The Tambien Group of Ethiopia: an early Cryogenian (ca. 800–735 Ma) Neoproterozoic sequence in the Arabian Nubian shield. Precambrian Research 149, 79–89.

Asrat A. (1997). Geology and geochemistry of the Negash pluton and their metalogenic significance, central Tigray.Unpublished. MSc Thesis, Addis Ababa University, Ethiopia,167pp.

Asrat, A., Barbey, P., and Gleizes, G. (2001). The Precambrian Geology of Ethiopia: a review, Africa Geoscience Review. 8: 271-288.

Asrat A., Gleizesc G., Barbeyi P., and Ayalew D. (2003). Magma emplacement and mafic–felsic magma hybridization: structural evidence from the Pan-African Negash pluton, Northern Ethiopia, Journal of Structural Geology. 25: 1451-1469.

Ayalew, T., Bell, K., Moore, J.M., and Parrish, R.R., 1990.U-Pb and Rb-Sr geochronology of the Western Ethiopian Shield. Geological Society America Bulletin 102, 1309-1316.

Avigad, D., Stern, R.J., Beyth, M., Miller, N., and McWilliams, M.O., 2007. Detrital zircon U-Pb geochronology of Cryogenian diamictites and Lower Paleozoic sandstone in Ethiopia (Tigray): Age constraints on Neoproterozoic glaciation and crustal evolution of the southern Arabian-Nubian Shield. Precambrian Research 154, 88-106.

Barker, A.J., (1998). Introductio to metamorphic textures and microstructures, 2nd ed. Stanley Thornes, United Kingdom, 263pp.

Berhe S.M. (1990). Ophiolites in northeast and east Africa: Implications for Proterozoic crustal growth, Journal Geological Society London. 147: 41-57.

Beyth M. (1972). The geology of central and western Tigre.PhD Thesis, University of Bonn, Germany, 155pp.

Beyth, M., Avigad, D., Wetzel, H. U., Matthews, A. & Berhe, S. M. (2003). Crustal exhumation and indications for snowball Earth in the East African Orogen: North Ethiopia and East Eritrea, Precambrian Research. 123: 187–201.

De Wit, M.J., 1981. Precambrian base metals. In: Chewaka, S., and de Wit, M.J. (eds.), Plate tectonics and metallogenesis: some guidelines to Ethiopian Mineral Deposits, Ethiopian Institute of Geological Surveys Bulletin 2, 65-82.

Gale, G.H., and Pearce, J.A., 1982. Geochemical patterns in Norwegian green stones, Canadian journal of earth science, 19(3); 385-397. doi:10.1139/e82-031.

Garcia, M. O., 1978. Criteria for identification of ancient volcanic arc. Earth and Planetary Science Letters.14: 147–165.

Garland, C.R., (1980). Geology of the Adigrat Area. Geological Survey of Ethiopia, Memoir1, 51 p.

Gebresillassie, S., 2009. Nature and characteristics of metasedimentary rock hosted gold and base metal mineralization in the Workamba area, central Tigray, northern Ethiopia. PhD thesis, Ludwig Maximilians, Munich University, Germany, 134p.

Gerra, S. 2000. A short introduction to the geology of Ethiopia. Chron. Rech. Min., 540: 3-10.

Irvine, T. N. and Barager,W. R. A., 1971. A guide to the chemical classification of the common volcanic rocks. Canadian Journal of Earth Science. 8: 523-548.

Johnson, P.R., Woldehaimanot, B., 2012. Development of the Arabian-Nubian Shield: perspectives on accretion and deformation in the northern East African Orogen and the assembly of Gondwana, .Geol. Soc. Lond.V206, p289-325.

Johnson, P.R., Andresen, A., Collins, A.S., Fowler, A.R., Fritz, H., Ghebreab, W., Kusky, T.,and Stern, R.J., 2011. Late Cryogenian–Ediacaran history of the Arabian–Nubian Shield: A review of depositional, plutonic, structural, and tectonic events in the closing stages of

the northern East African Orogen. Journal of African Earth Sciences,Volume 61, Issue 3,167- 232.

Kazmin V. (1972).The geology of Ethiopia.Ethiopian Institute of Geological Surveys. Note No. 821.

Kazmin, V. (1973). The geological map of Ethiopia, 1:2,000,000. Ethiopian Institute of Geological Surveys, Addis Ababa, Ethiopia.

Kazmin,V., Shiferaw, A., and Balcha, T., 1978. The Ethiopian basement and possible manner of evolution, Geologische Rundschau 67, 531-546.

Kennedy, W.Q. (1964). The Structural differentiation of Africa in the Pan-African (±500 m.y). Tectonic episode: Res. Inst.Afri. Geol., University of Leeds, 8th ann. Rep., p. 48-49.

Kroner, A., (1979). Pan African crustal evolution. Updated and modified version of paper presented, Cairo, Egypt, October. Episode, Vol. 1980, No.2.

Kroner, A.,Linnebacher, P., Stern, R.J., Reischmann, T., Manton, W., and Hussein, I.M., (1991). Evolution of Pan-African island arc assemblages in the southern Red Sea Hills, Sudan, and in south-western Arabia as exemplified by geochemistry and geochronology. Precambrian Research 53, 99-118.

Kroner, A.,Stern, R.J.,(2005), Pan-African Orogeny,Vol.1, Amsterdam: Elsevier.Sudan, Geologische Rundschau. 87: 150–160.

McDonough, W.F., Sun, S., 1995. The composition of the Earth. Chemical Geology 120, 223e253.

McWilliams (1981).Palaeomagnetism and Precambrian tectonic evolution of Gondwana. In Precambrian Plate Tectonics, ed. A Kroner, pp. 649-87. Amsterdam: Elsevier.

Mengesha Tefera., Tadiwos Chernet and Workineh Haro. (1996). Explanation of the Geological map of Ethiopia.Ethiopian Institute of Geological Survey.

Miller, N.R., Alene, M., Sacchi, R., Stern, R., Conti, A., Kröner, A., Zuppi, G., (2003).Significance of the Tambien Group (Tigre.N. Ethiopia) for Snowball Earth Events in the Arabian–Nubian Shield. Precambrian Research 121, 263– 283.Miller, N.R., Avigad, D., Stern, R.J. and Beyth, M. (2011).The Tambien Group, Northern Ethiopia (Tigre), Geological Society of London. 36: 263-276.

Passchier, C.W. and Trouw, R.A.J. (2005).Microtectonics. Springer-Verlag, Berlin, 289 pp.

Pearce, J.A., Cann, J.R., 1973. Tectonic setting of basic volcanic rocks determined using trace element analysis. Earth and Planetary Science Letters 19, 290–300.

Pearce, J.A., 1982. Trace element characteristics of lavas from destructive plate boundaries. In: Thorpe, R.S. (Ed.), Andesites, Orogenic Andesites and Related Rocks. John Wiley, New York, pp. 525e548.

Rollinson, H.R. (1993). Using geochemical data: evaluation, presentation, interpretation: Routledge.

Sifeta, K., Roser, B.P., Kimura, J.I., (2005). Geochemistry, provenance, and tectonic setting of Neoproterozoic metavolcanic and metasedimentary units, Werri area, Northern Ethiopia. Journal of African Earth Sciences 41, 212–234.

Stern, R.J., (1994). Arc assembly and continental collision in the Neoproterozoic East African Orogen: implications for the consolidation of Gondwanaland. Annual Reviews of Earth and Planetary Sciences 22, 319–351.

Stern, R.J., (2002). Crustal evolution in the East African Orogen: a neodymium isotopic perspective. Journal of African Earth Sciences 34, 109–117.

Stern, R.J., Johnson, P.R., Kr¨oner, A., Yibas, B., 2004. Neoproterozoic ophiolites of the Arabian–Nubian shield. In: Kusky, T.M. (Ed.), Precambrian Ophiolites and Related Rocks, vol. 13. Developments in Precambrian Geology, pp. 95–128.

Stern, R.J., Kroner, A., (2005). Pan-African Orogen.Encyclopedia of Geology, v. 1. Elsevier, Amsterdam.

Swanson-Hysell, N.L., Maloof, A.C., Condon, D.J., Jenkin, G. R.T., Alene, M., Tremblay M .M. Tesema, T., Rooney, A. D., & Haileab,B.,2015. Stratigraphy and geochronology of the Tambien Group, Ethiopia: Evidence for globally synchronous carbon isotope change in the Neoproterozoic, Geology, published, doi:10.1130/G36347.1.

Tefera, T. (1996). Structure across a possible intra-oceanic suture zone in low-grade Pan African rocks of northern Ethiopia, Journal of African Earth Sciences. 23: 575-381.

Tefera, T., Suzuki, K., Hoshino, M., 1997. Chemical Th-U-total Pb ischron age of zircon from the Mereb granite in northern Ethiopia. Journal Earth Planetary Science Nagaya University 44, 21-27.

Tefera, T., Hoshino, M., Sawada, Y. (1999).Geochemistry of low grade metavolcanic rocks from the Pan-African of the Axum area, northern Ethiopia, Precambrian Research. 99:101–124.

Tefera, T., Hoshino, M., Suzuki, K., and Iisumi, S., 2000. Sm-Nd, Rb-Sr, and Th-U-Pb zircon ages of syn- and post-tectonic granitoids from the Axum area of northern Ethiopia. Journal of African Earth Sciences 30, 313-327.

Teklay, M., Kröner, A., Mezger, K., and Oberhansli, R., (1998). Geochemistry, Pb-Pb single Zircon ages and Nd-Sr isotope composition of Precambrian rocks from southern and Eastern Ethiopia: implications for crustal evolution in East Africa. Journal of African Earth Sciences, 26, 207-227.

Teklay, M., Kro¨ner, A. & Metzger, K. (2001). Geochemistry, geochronology and isotope geology of Nakfa intrusive rocks, northern Eritrea: products of a tectonically thickened Neoproterozoic arc crust. Journal of African Earth Sciences, 33, 283–301.

Timothy M. Kusky, Mohamed Abdelsalam, Robert J. Stern, Robert D. Tucker, (2003). Evolution of the East African and related orogens, and the assembly of Gondwana. Precambrian Research 123 (2003) 81–85.

Vail, J.R., 1985. Pan-African (late Precambrian) tectonic terrans and the reconstruction of the Arabian-Nubian Shield. Geology 13, 839-842.

Winter John D., (2001). An introduction to igneous and metamorphic petrology, United State of America, 634pp.

Wood, D.A., 1980. The application of a Th–Hf–Ta diagram toproblems of tectonomagmatic classification and to establishing the nature of crustal contamination of basaltic lavas of the BritishTertiary volcanic province. Earth and Planetary Science Letters 50,11–30.

List of Appendix I

Appendix 1Measured data of different structural elements

No	Measured structural element	strike	Dip amount & direction	Location	Lithological Unit
1	S0	035	50NW	0498377E,1520201N	Meta basic
2	S1	030	45NW	0498160E,1522175N	Met volcanic clast
3	S1	063	65SE	0498063E,1522447N	Massive tuff
4	S1	060	30NW	0497244E,15230309N	Foliated tuff
5	S0	060	65SE	0497739E,1525456N	massive tuff
6	S1	020	60NW	0497877E,1521154N	Metabasic
7	Qrz vein	025	55NW	0497877E,1521154N	Metabasic
8	S1	025	40NW	0496679E,1522175N	Metabasic
9	S1	035	55NW	0495970E,1520078N	Metabasic
10	S1	028	40NW	0498297E,1524287N	Metaandesite with intercalated tuff
11	S0	030	45NW	0497089E,1524560N	Metabasic
12	S0	028	50NW	0497089E,1524560N	Metabasic
13	S0	025	35NW	0494830E,1524760N	Metabasic
14	S1	025	45NW	04960187E,1520081N	Metabasic
15	S1	035	40NW	0498496E,1522669N	Foliated tuff
16	S1	050	45NW	0498912E, 1523801N	Metabasic
17	S1	025	40NW	0499108E, 1525170N	Metaandesite with intercalated tuff
18	S1	035	65NW	0499108E, 1525170N	Metaandesite with intercalated tuff
19	S1	032	35NW	0498263E,1525777N	Metabasic with intercalated tuff
20	S0	040	70NW	0498197E,1526081N	Metabasic
21	S1	028	25NW	0499050E,1525841N	Meta volcanic clast
22	S0	025	35NW	0499088E, 1525901N	Meta volcanic clast
23	S0	038	55NW	0499051E, 1527516	Metabasic
24	S1	035	35NW	0496601E,1527026N	Slate
25	S1	055	65NW	0497053E,1527803N	Graphitic slate
26	S1	045	45NW	0496653E,1527806N	Graphitic slate
27	S0	032	75NW	0495206E, 1527989N	Metalimstone
28	S0&S1 (composite)	035	70NW	0498494E, 1527374N	Layers of Tuff with color variation
29	S0	028	55NW	0498473E,1527390N	Metabasic
30	S0	035	54NW	0498473E,1527390N	Metabasic
31	S1	032	50NW	0499173E,1526998N	Metabasic with intercalated tuff
32	S1	038	50NW	0499551E,1526567N	Metabasic
33	S1	027	42NW	0495045E,1526857N	Meta volcanic clast
34	S0	024	55NW	04950165E,1526226N	Metabasic
35	S1	035	24NW	0498870E,1523159N	Meta volcanic clast
36	S1	025	45NW	0499495E,1524161N	Tuff
37	S0	055	40NW	0500045E,1524081N	Massive tuff
38	S1	034	65NW	0500631E,1523728N	Meta volcanic clast

39	S0	018	75SE	0500982E,1523621N	Meta volcanic clast
40	S1	035	40NW	0501529E,1523555N	Metabreccia
41	S0	024	55NW	0502605E,1522515N	Metabasic
42	S1	020	45NW	0502004E,1520019N	Metabreccia
43	S1	025	30NW	0503971E,1521677N	Phyllite

No	Measured structural element	strike	Dip amount & direction	Location	Lithological Unit
44	S1	038	45NW	0504578E,1521294N	phyllite
45	S2	115	56 SE	0504578E,1521294N	phyllite
46	S1	030	40NW	0503208E,1520422N	Metabasic
47	S1	034	40NW	0503208E,1520422N	Metabasic
48	S1	020	35NW	0504369E,1522607N	Metabreccia
49	S0	025	45NW	0504927E,1525627N	Metabasic
50	S1	035	70SE	0504196E,1522253N	phyllite
51	S1	028	50NW	0504116E,15212187N	phyllite
52	S2	105	45SE	0504116E,15212187N	phyllite
53	S1	033	24NW	0503740E,1520250N	Slate
54	S1	025	42NW	0503690E,1520306N	Slate
55	S0	018	34NW	0499081E,1520977N	Metabasic
56	S1	034	55NW	0501834E,1521370N	Metabasic
57	S0	030	45NW	0497089E,1524560N	Metabasic
	Measured structural element	strike	Dip amount & direction	Location	Lithological Unit
58	Joints	020	70SE	0498377E,1520201N	Metabasic
59	Joint	018	80SE	0497877E,1521154N	Metabasic
60	Joint1	010	65 SE	0496679E,1522175N	Metabasic
61	Joint2	150	86NE	0496679E,1522175N	Metabasic
62	Joint	030	85SE	0498912E, 1523801N	Metabasic
63	Joint	015	Vertical	04960187E,1520081N	Metabasic
64	Joint	030	85SE	0498263E,1525777N	Metabasic
65	Joint1	150	75NE	0499050E,1525841N	Meta volcanic clast
66	Joint2	020	85SE	0499050E,1525841N	Meta volcanic clast
67	Joint	010	70 SE	0499088E, 1525901N	Meta volcanic clast
68	Joint	060	70NW	0495206E, 1527989N	Metalimstone
69	Joint	010	75SE	0499173E,1526998N	Metabasic
70	Joint	018	65SE	0501834E,1521370N	Metabasic
71	Joint	015	80SE	0503208E,1520422N	Metabasic
72	Joint	025	80NW	0495970E,1520078N	Metabasic
73	Joint	018	86SE	0498297E,1524287N	Metabasic
74	Joint	034	vertical	0499551E,1526567N	Metabasic
75	Joint	020	85SE	04950165E,1526226N	Metabasic
76	Measured structural element	strike	Dip amount & direction	Location	Lithological Unit which is Vein found

77	Qrz vein	025	55NW	0497877E,1521154N	Metabasic
78	Mica vein	055	vertical	0495206E, 1527989N	Metalimstone
79	Qrz vein	030	45NW	0496601E,1527026N	Slate
80	Qrz vein	015	vertical	0503208E,1520422N	Metabasic
81	Qrz vein	020	vertical	0502004E,1520019N	Metabreccia(hematized phyllite)
82	Qrz vein	025	vertical	0502004E,1520019N	Metabreccia(hematized phyllite)
83	Qrz vein	015	vertical	0503208E,1520422N	Metabasic

No	Measured structural element	Plunge	Trend	Location
1	Fold axis (FA)	05	165	0499506E,1527969N
2		10	190	0499508E,1528008N
3		0 8	184	04999508E,1528008N
4		08	195	0499506E,1527980N
5		06	200	0499506E,1527980N
6		07	175	0499603E,152802N
7		35	065	0503208E, 1520422N
	Measured structural element	Strike	Dip amount & direction	Location
8	Fold Axial plane	185	75SE	0499506E,1527969N
9		195	55SE	0499508E,1528008N
10		190	60SE	04999508E,1528008N
11		190	70SE	0499506E,1527980N
12		180	54SE	0499506E,1527980N
13		195	50SE	0499603E,152802N
14		175	65SE	0503208E, 1520422N
Type of Structural	Plunge	Trend	Location	Note
Lineation	7	155	0504369E,1522607N	Phyllite
	10	145	0504369E,1522605N	Phyllite
	8	150	0504116E,1522187N	Phyllite
	6	155	0504196E,1522253N	Crenulation lineation in phyllite
	8	150	0504196E,1522253N	Crenulation lineation in phyllite

Appendix 2 Abbreviations

Chl Chlorite
Ep Epidote

Act	Actinolite
Cal	Calcite
Kfs	k-feldspar
Ms	Muscovite
Ol	Olivine
Gr	Graphite
Px	Pyroxene
Pl	Plagioclase
Qtz	Quartz
Ser	Sericite
Tr	Tremolite
MV	Metavolcanic